1990 XXXXXX/DISSERTATION

The Effect of Irradiation on Bone Remodelling and the Structural Integrity of the Vertebral Column

Kristin Natvig Swenson

AFIT Student Attending: University of Cincinnati

AFIT/CI/CIA-90-027D

AFIT/CI
Wright-Patterson AFB OH 45433-6583

GENERAL INSTRUCTIONS FOR COMPLETING SF 298

The Report Documentation Page (RDP) is used in announcing and cataloging reports. It is important that this information be consistent with the rest of the report, particularly the cover and title page. Instructions for filling in each block of the form follow. It is important to ***stay within the lines*** to meet ***optical scanning requirements***.

Block 1. Agency Use Only *(Leave blank)*.

Block 2. Report Date. Full publication date including day, month, and year, if available (e.g. 1 Jan 88). Must cite at least the year.

Block 3. Type of Report and Dates Covered. State whether report is interim, final, etc. If applicable, enter inclusive report dates (e.g. 10 Jun 87 - 30 Jun 88).

Block 4. Title and Subtitle. A title is taken from the part of the report that provides the most meaningful and complete information. When a report is prepared in more than one volume, repeat the primary title, add volume number, and include subtitle for the specific volume. On classified documents enter the title classification in parentheses.

Block 5. Funding Numbers. To include contract and grant numbers; may include program element number(s), project number(s), task number(s), and work unit number(s). Use the following labels:

C	-	Contract
G	-	Grant
PE	-	Program Element
PR	-	Project
TA	-	Task
WU	-	Work Unit Accession No.

Block 6. Author(s). Name(s) of person(s) responsible for writing the report, performing the research, or credited with the content of the report. If editor or compiler, this should follow the name(s).

Block 7. Performing Organization Name(s) and Address(es). Self-explanatory.

Block 8. Performing Organization Report Number. Enter the unique alphanumeric report number(s) assigned by the organization performing the report.

Block 9. Sponsoring/Monitoring Agency Name(s) and Address(es). Self-explanatory.

Block 10. Sponsoring/Monitoring Agency Report Number. (If known)

Block 11. Supplementary Notes. Enter information not included elsewhere such as: Prepared in cooperation with ...; Trans. of ...; To be published in .... When a report is revised, include a statement whether the new report supersedes or supplements the older report.

Block 12a. Distribution/Availability Statement. Denotes public availability or limitations. Cite any availability to the public. Enter additional limitations or special markings in all capitals (e.g. NOFORN, REL, ITAR).

- **DOD** - See DoDD 5230.24, "Distribution Statements on Technical Documents."
- **DOE** - See authorities.
- **NASA** - See Handbook NHB 2200.2.
- **NTIS** - Leave blank.

Block 12b. Distribution Code.

- **DOD** - Leave blank.
- **DOE** - Enter DOE distribution categories from the Standard Distribution for Unclassified Scientific and Technical Reports.
- **NASA** - Leave blank.
- **NTIS** - Leave blank.

Block 13. Abstract. Include a brief *(Maximum 200 words)* factual summary of the most significant information contained in the report.

Block 14. Subject Terms. Keywords or phrases identifying major subjects in the report.

Block 15. Number of Pages. Enter the total number of pages.

Block 16. Price Code. Enter appropriate price code (NTIS only).

Blocks 17. - 19. Security Classifications. Self-explanatory. Enter U.S. Security Classification in accordance with U.S. Security Regulations (i.e., UNCLASSIFIED). If form contains classified information, stamp classification on the top and bottom of the page.

Block 20. Limitation of Abstract. This block must be completed to assign a limitation to the abstract. Enter either UL (unlimited) or SAR (same as report). An entry in this block is necessary if the abstract is to be limited. If blank, the abstract is assumed to be unlimited.

ABSTRACT

Swenson, Kristin Natvig, Ph.D., Nuclear Engineering (Medical Physics) Ph.D. Program, University of Cincinnati, 1990. The Effect of Irradiation on Bone Remodelling and the Structural Integrity of the Vertebral Column.

The effects of therapeutic levels of radiation on the axial properties of the primate vertebral column were studied. Seven male rhesus monkeys (Macaca mulatta) were irradiated with a single dose of 1300 cGy to the specific lumbar vertebrae of L2, L3, and L4. Three additional animals served as controls. Radiographs were taken before the radiation treatment and just prior to sacrifice to determine density changes in the bone. The animal subjects were sacrificed 105 days following the radiation exposure. Biomechanical testing was completed on lumbar levels 2 and 3 to identify changes in strength characteristics following radiation treatment. Histomorphometric analysis of lumbar vertebrae level 4 was completed to identify volume and surface density changes as well as cellular changes. Tetracycline, dicarbomethylaminomethyl fluorescein (DCAF), and xylenol orange were used as bone labeling agents to aid in the histomorphometry and to obtain dynamic parameter changes. Finally, trabecular pattern measurements were completed on lumbar level 4.

The histomorphometry indicated significant decreases in bone volume and surface density of bone for selected regions. Osteoid volume increased in three of the four regions, and osteoid surface density increased in all four analytical regions (anterior, posterior, inferior, and superior). Adjusted appositional rate increased in the posterior region, as measured between the first two labels and the

THE EFFECT OF IRRADIATION ON BONE REMODELLING AND THE STRUCTURAL INTEGRITY OF THE VERTEBRAL COLUMN

A Dissertation submitted to the

Division of Graduate Studies and Research
of the University of Cincinnati

in partial fulfillment of the
requirements for the degree of

DOCTOR OF PHILOSOPHY

in the Department of Mechanical, Industrial and Nuclear Engineering
of the College of Engineering

1990

by

Kristin Natvig Swenson

B.S., University of Iowa, 1982

M.S., Wright State University, 1987

Committee Chair: Dr. Roy Eckart
Committee Co-Chair: Dr. David Denman

last two labels on the irradiated animal subjects. Compression testing on the vertebral centrum resulted in no significant differences between the treatment and control groups. Trabecular pattern measurement indicated significant differences in the amount of horizontal supporting trabeculae, with a large decrease for the irradiated animal subjects. Also a decrease in the number of vertical trabeculae in the upper quadrant was observed. The radiographs did not indicate any differences between the control and the irradiated animal subjects. The above results indicate that therapeutic levels of radiation may bring changes upon the skeletal system, specifically decreased bone and/or surface volume, and increased activation frequency and bone formation. Strength is maintained in the trabecular structure. by compromising the horizontal trabeculae.

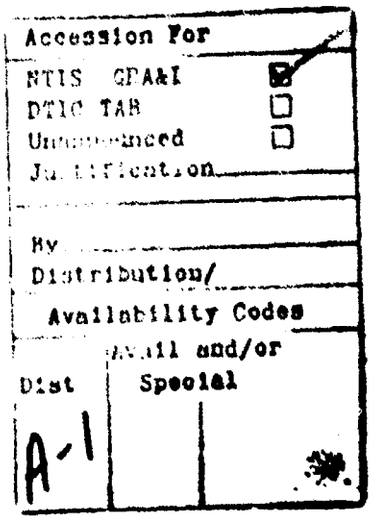

ACKNOWLEDGEMENT

The author would like to express her appreciation to the personnel of the Biomechanics Branch of the Biodynamics and Bioengineering Division and the Veterinary Science Branch of the Toxic Hazards Division of the Armstrong Aerospace Medical Research Laboratories (AAMRL), and the Radiation Therapy Department of the Wright Patterson Medical Center (SGHRT), Wright-Patterson Air Force Base, Ohio for their support and assistance.

In particular, I would like to thank:

Dr. Leon Kazarian, Branch Chief, Biodynamics Effects Branch, for his influence and inspiration on this project and for making the laboratory resources available to me.

Mr. Edward Eveland of the Biodynamics Effects Branch, for his technical expertise and assistance in completing the Histomorphometric Analysis.

Dr. James Cooper, Ms. Brenda Schimmel, and Mr. Tim Bausman of the Veterinary Science Branch for their time and professional expertise with the care and treatment of the animal subjects.

Dr. Daniel Hommel and Captain Kenneth Wohlt of the Radiation Therapy Department for their technical and professional help with the dose administration and the dosimetry.

And especially to my husband, Kevin, without whose help and encouragement I could not have completed this program and project so successfully.

TABLE OF CONTENTS

ABSTRACT iii

ACKNOWLEDGEMENTS v

TABLE OF CONTENTS vi

LIST OF FIGURES vii

LIST OF TABLES ix

INTRODUCTION 1

EXPERIMENTAL PROCEDURES AND RESULTS 8

- Experimental Animals 8
- In Vivo Samples, Measurements and Administration 9
- Necropsy and Tissue Collection 10
- Dose Administration and Dosimetry 12
- Blood Analysis 24
- Biomechanical Testing 25
- Histomorphometry 32
- Trabecular Pattern Measurement 56
- Densitometry of Radiographs 60

DISCUSSION 64

SUMMARY 71

REFERENCES 75

APPENDIXES 82

LIST OF FIGURES

1. Transport of animals from the veterinary facility to the radiation therapy department..... 13

2. Rhesus monkey in position in linear accelerator treatment room..... 13

3. Radiograph of anterior-posterior treatment field from simulator set up..... 14

4. Radiograph of lateral view treatment field from simulator set up..... 14

5. Isodose curves calculated from the treatment plan showing view of sagittal lumbar spine..... 16

6. Isodose curves calculated from the treatment plan showing superior view of anterior to posterior irradiation..... 17

7 Calibration curve of lithium-fluoride thermoluminescent dosimeters..... 19

8. Placement of the thermoluminescent dosimeters on the left anterior portion of the vertebrae..... 20

9. Placement of thermoluminescent dosimeters on vertebral bodies with dose distribution for lumbar levels 2, 3 and 4..... 22

10. Material Testing System used for vertebral centrum compression tests with test specimen in place with polymethylmethacrylate pots..... 27

11. Typical load test on a vertebral centrum showing the method used to determine compression strength parameters from force/displacement curves..... 28

12. Lumbar four vertebrae embedded in polymethylmethacrylate and cut in half in preparation of thin slicing on precision bone saw..... 34

13. Polycut precision bone saw for cutting the embedded vertebral sections to 10 micron thick slices..... 34

14. Lumbar four vertebral section mounted on slide..... 36

15. Zeiss photomicroscope and Videoplan computer system used for histomorphometric analysis..... 36

16. View of the microscopic measurement field..... 37

17. Lumbar four vertebral centrum midsagittal section illustrating location of histomorphometric analysis sites..... 38

18. Trabecular pattern of bone with lining cells and osteoid which is the darkened area marked by arrows..... 40

19. Osteoclast with multiple nuclei identified with arrows..... 41

20. Osteochrome evident under ultraviolet light. Two labels (tetracycline and xylenol orange) are identified by arrows..... 42

21. Osteochrome under ultraviolet light displaying all four bone labels given (tetracycline, DCAF, xylenol orange and againtetracycline)..... 43

22. Trabecular pattern measurement analysis sites..... 57

23. Anterior-Posterior radiograph with gradient aluminum wedge used for densitometry..... 61

24. Lateral radiograph with gradient aluminum wedge used for densitometry..... 61

LIST OF TABLES

1. Subject Identification, Birth dates, Weights and Treatment Group..... 10

2. Vertebral Centrum Compression Test Results, Mean (X), Standard Deviation (S), and Sample Number (N)..... 30

3. Vertebral Centrum Trabecular Bone Histomorphometric Analysis Parameters..... 44

4. Bone Histomorphometry, Lumbar Four Analysis, Superior Region, Mean (X), Standard Deviation (S), and Sample Number (N)... 47

5. Bone Histomorphometry, Lumbar Four Analysis, Inferior Region, Mean (X), Standard Deviation (S), and Sample Number (N)... 48

6. Bone Histomorphometry, Lumbar Four Analysis, Anterior Region, Mean (X), Standard Deviation (S), and Sample Number (N)... 49

7. Bone Histomorphometry, Lumbar Four Analysis, Posterior Region, Mean (X), Standard Deviation (S), and Sample Number (N)... 50

8. Bone Histomorphometry, Lumbar Four Analysis Bone Labeling Parameters, Superior Region, Mean (X), Standard Deviation (S), and Sample Number (N)..... 52

9. Bone Histomorphometry, Lumbar Four Analysis Bone Labeling Parameters, Inferior Region, Mean (X), Standard Deviation (S), and Sample Number (N)..... 53

10. Bone Histomorphometry, Lumbar Four Analysis Bone Labeling Parameters, Anterior Region, Mean (X), Standard Deviation (S), and Sample Number (N)..... 54

11. Bone Histomorphometry, Lumbar Four Analysis Bone Labeling Parameters, Posterior Region, Mean (X), Standard Deviation(S), and Sample Number (N)..... 55

12. Trabecular Pattern Results, Lumbar Four, Mean (X), Standard Deviation (S), and Sample Number (N)..... 58

13. Density percentage ranges for Radiographic Densitometry Measurements..... 62

INTRODUCTION

The skeletal system is composed of dynamically changing tissues which adapt in response to external and internal factors including workload, diet, hormones, disease, and gravity. During normal activity, the magnitude and orientation of the strains imposed on the skeletal system are a result of a complex interaction between external forces and muscular activity. In the absence of physical activity, or due to disease, osteolysis occurs which results in bone resorption. Previously thought to be resistant to doses of radiation, bone has recently been shown to be relatively radiosensitive (Ergun and Howland 1980). An increase in spontaneous fracture incidence following irradiation was observed as early as 1926, before radiation therapy was utilized to the extent that it is today for cancer therapy (Ewing 1926). Radiation induced changes in bone several years after radiation therapy are described as irregular, lytic, having transverse fissures, and increased radiolucency confined to the irradiated volume (Howland et al. 1975). Sengupta and Prathap (1973) described three cases seven years post irradiation. All three cases had widespread osteoporosis with two individuals exhibiting patchy sclerosis. One individual had a fracture of the humerus due to the osteoporosis. While osteoporosis and subsequent fracture occurrence have a latency period of years, the histological effect, as observed by osteoblast and osteoclast changes, can be observed as early as four weeks post radiation. (Dalinka et al. 1974, Rafii et al. 1988, and Albrecktsson et al. 1980b). True radiation induced osteonecrosis (irreversible death of bone) rarely occurs (Ergun and Howland 1980).

The primary result of radiation treatment of bone is atrophy and as described by Ergun and Howland (1980), is due to primarily

three reasons: 1) absence of essential nutrients, 2) interference with nutrient uptake and normal cellular stimulation and 3) damage to the vascular system supplying the bone tissue. Thus, the two primary factors to be considered for the observed post radiation bone atrophy are the vascular changes and the bone changes at the cellular level. It is not known which of these two dominates the resultant damage to the bone, but both have a major role. (Ergun and Howland 1980) More than likely it is a combination of the two, as the vascular supply delivers the nutrients needed for the bone remodelling sequence to proceed as normal (Dambrain et al. 1988), and the bone resorption has been associated with dilated blood vessels and reduced blood flow (Albrecktsson 1980a). However, the vascular reaction following irradiation is very hard to analyze due to the presence and opacity of the bone tissue (Albrektsson et al. 1985). The pattern of the individual trabeculae play a very important role in the response of the bone to mechanical loading. Whereas cortical bone is very compact, dense and primarily resists bending forces, trabeculae or cancellous bone is of a lattice structure made of supporting framework of lamellar bone filled with bone marrow tissue. The construction or makeup of trabecular bone is optimum in responding to any type of compressive loading. Thus, the logic behind the locations of the trabecular bone in the human body: vertebra, pelvis and the femoral head and neck. Cortical bone is primarily in the long bones or appendages and the outer walls of all bones of the mammal. This also helps explain how hip fractures can easily occur in osteoporotic individuals: the femur is under a bending or torsional loading situation along with predominant loss of trabecular bone and the fact that it responds best under compressive loads and not bending loads, results in a fracture. (Ergun and Howland 1980; and Van Audekercke and Martens 1984)

This process of bone activity at the cellular level is termed modelling or remodelling. Modelling signifies the resorptive and formative process in association with elongation of growth: the forming and shaping of a growing bone. Remodelling, on the other hand, refers to the processes of resorption and formation that continue after growth has taken place (Frost 1969; and Frost 1983).

Remodelling maintains skeletal integrity by repairing and renewing damaged and senescent bone before it hinders the skeletal framework function. The skeletal system is sensitive to the demands made upon it and is able to adjust its structure accordingly. In other words, bone is able to respond to internal strains and pass along information to the osteoprogenitor cells for appropriate action, that being differentiation of osteoblasts from osteoprogenitor cells at the site where new bone is required to strengthen the structure, and of osteoclasts to the location where redundant bone is found (Albright and Brand 1979). Remodelling occurs in individual "groups" of bone cells that respond to a given stimulus (Parfitt 1983a; and Frost 1983). These remodelling groups or packets are referred to as Basic Multicellular Units (BMUs) (Frost 1983a) or Bone Structural Units (BSUs) (Parfitt 1983a). The BMUs react to some yet unknown stimulus, that causes activation of the osteoprogenitor cells producing daughter cells, those being either osteoclasts or osteoblasts. The osteoclasts appear first and actively resorb bone, approximately 0.05 μm^3 per BMU (Frost 1969). Osteoclasts are large multinucleated cells found within Howship's lacunae or areas erroded away by the osteoclasts. Under microscopic examination osteoclasts have a ruffled border and therefore larger surface area, to infiltrate and disintegrate bone. The percent of resorbing surface of trabecular bone at any given time for a human is 1.2%, twice that of cortical bone. During resorption the solid mineral is solubized and is transferred via the osteoclast to the extra cellular fluid (ECF). Contact of the bone with the ECF is strictly through osteoclasts, osteoblasts or lining cells, which are quiescent osteoblasts lining the bone surface. Next, osteoblasts appear and replace with new bone that which the osteoclasts have previously removed. Formation occurs only in those areas of bone that have undergone resorption (Frost 1963). Six percent of the total trabecular bone surface is in the formation phase, again twice as much as the cortical bone. The rest of the trabecular bone surface (92.8%) is in an inert phase. Bone formation occurs in two steps: matrix formation (osteoid or unmineralized bone) and mineralization. The time delay or mineralization lag time between the initial laying down of the osteoid and mineralization is about 10-

20 days. Mineralization does not occur all at once. Primary mineralization is due to the osteoblasts, and only about 70% of the maximum mineral density is reached. After a few days the resting osteoblasts or lining cells increase the mineral density to 95%. Greater mineralization than this is known as the disease state osteopetrosis (Parfitt 1983a). A great amount of information is learned from in vivo bone labels known as osteochromes. Certain chemical agents such as tetracycline can become incorporated irreversibly into the bone matrix as mineralization occurs. Under ultraviolet light these osteochromes fluoresce and a permanent marker remains. When these markers are administered two weeks hence, measurements may be made that correspond to bone growth, resulting in a dynamic measurement parameter.

This sequence of events taking place during remodelling is denoted by Activation-Resorption-Formation (A-R-F). The amount of time that this sequence takes is referred to as sigma. Duration of formation and resorption differ among species and between different parts of the skeleton (Podenphant and Engel 1987). The duration of human formation is 76 days, while that of a monkey is 55 days. The duration of resorption is 15.1 days in man and 13.0 days in monkeys. Sigma for the entire sequence also includes a quiescent period of 0-20 days between the resorption and formation phases of the sequence. Thus, for man, the total sigma can range between 95 and 125 days (Parfitt 1983a).

The bone remodelling sequence of A-R-F has not been observed to decrease in all aspects but the osteoblasts (formation) seem to be particularly sensitive to radiation (Ergun and Howland 1980; and Cox and Moss 1986). Sengupta and Prathap (1973) report that osteoblasts virtually disappear, but that their activity is not completely suppressed even at 10,000 cGy(rad). Growing bone which is primarily in the modelling stage (thus mostly osteoblastic activity), does not reach its expected length following radiation. This effect of radiation on growing bone substantiates the observed response of the osteoblasts to radiation (Rubin 1959; Barnhard and Geyer 1962; and Vaughan 1968). Alkaline phosphatase activity, which is associated with osteoblastic activity, has also been observed

to decrease following radiation treatment (Babicky and Kolar 1966; Engstrom 1987; and Sams 1965). However, if the osteoblasts are more sensitive than osteoclasts, the normal A-R-F sequence will be abnormal and resorption will be greater than the formation due to the effect on the osteoblasts. Most likely this will result in less trabecular volume, narrowing of the trabeculae and an increase in the marrow space. Porosity can increase (Maeda et al. 1988) as well as a loss of the structural components. This could affect the resulting compressive strength of the vertebrae, depending on which trabecular elements are compromised. As late as 10 weeks post radiation treatment, osteocyte lacunae still lacked outer demarcation at doses of 1500 cGy to the long bones of rabbits. Osteocytes, or end stage cells, are radioresistant after doses of 40 Gy irradiation (Jacobsson 1985c, 1987).

With this decrease in osteoblastic activity, osteoclastic activity has been observed to increase, resulting in empty lacunae. Results by Maeda and coworkers (1988) suggest that both osteoblastic and osteoclastic activity were suppressed in rats subjected to a single dose of 3500 cGy to the right femur. As early as 4 weeks post radiation, mature bone appeared slightly remodelled in the rabbits. By 6 weeks bone resorption was more apparent and by 10 weeks new bone formation was observed. (Albrecktsson et al. 1980b) Changes in acid phosphatase, which is associated with changes in osteoclastic activity, have been observed to increase during the experimental period and return to normal after 30 days (Engstrom 1987). Some studies utilizing rats and mice as subjects report no effect on formation at all, thus no osteoblastic impairment, but bone remodelling alterations were only due to changes in bone resorption activities (Anderson et al. 1979; and Albrektsson et al. 1980). Jee (1984) similarly observed that effects on the osteoclasts were directly related to the vascular system. Differentiation of osteoclasts was due to decreased bone blood perfusion which induced hypoxia thus stimulating differentiation.

Some studies have shown that the bone remodelling dynamics are altered but that they can return to normal after a period of time. Bures and Wuehrmann (1968) wrote that the remodelling observed

changes in rats' mandibles and tibias returned to normal 45 days post radiation therapy (4500 and 9000 cGy dose). Aitasalo and Neva (1985) reported changes in the number of trabeculae and porosity that were reversible 6 to 12 months later. Studies concerning regeneration of bone also substantiated a return to the norm in bone remodelling (Amsell and Dell 1972; Jacobsson et al. 1985a, 1985b, 1985d; and Saha 1985).

Changes in bone growth have been observed experimentally at irradiation treatment levels of 500 cGy (Jacobsson et al. 1985a), but most definitely at levels above 2400 cGy (Aronson et al. 1976; Maeda et al. 1988; Spencer et al. 1988; and Jacobsson et al. 1985b,1985c). Radiographically demonstrable atrophic changes begin to appear at 4000 cGy(rem) absorbed dose and become severe up to 10,000 cGy(rem) absorbed dose (Howland et al. 1975; Ergun and Howland 1980; and Spencer et al. 1988). Observation of these radiographs by the human eye can only detect changes after a 30-60% reduction in the calcium content in the vertebral column (Crone-Munzebrock 1987; and Ergun and Howland 1980).

Deformations in the spine due to childhood radiation treatments have been determined to be dependent on several factors: 1) length of the spine irradiated, 2) radiation dose and dose gradient, 3) age of patient, 4) time duration since treatment, and 5) post treatment medical care (Parker and Berry 1976). These concerns can also be applied to radiation treatment of adult bone.

The primary objectives of this research were to quantitate the effects of therapeutic levels of radiation on the mechanical properties and the cellular changes of the vertebral bodies. Quantitation was accomplished through four methods: histomorphometry, compression tests, trabecular pattern measurement and densitometry. Histomorphometric analysis (or the measurement of cellular activity) of bone remodelling parameters exposed the activity at the cellular level. This cellular analysis can provide the underlying information that is responsible for the more obvious results or complications of radiation therapy. Trabecular bone is a better indicator of osteoporosis as bone turnover is much faster than in cortical bone (Leichter et al. 1987). The vertebral centrum

compression testing was completed to quantitate the gross strength changes. These two methods are commonly used to assess cellular and strength changes resulting from mechanical stresses. The trabecular pattern measurement was completed to help support the results from the biomechanical testing and the histomorphometry with information about the individual trabecula within the vertebral column.

Density changes were observed through radiographs. Histomorphometry and compression tests are destructive tests and cannot be used in clinical practice, but in research can tell us a great deal. Density measurements however, can be used in a clinical environment and thus compared with these experimental results. Changes in bone density observed allow one to establish a response relationship for the acute changes observed in human patients. This is clinically important as it will help predict which radiation therapy patients may be at substantial risk for future complications. Once bone formation is hindered and bone density lost, osteoporosis can result with fracture or radiation induced osteonecrosis likely to follow. (Cox and Moss 1989; and Sengupta and Prathap 1973)

EXPERIMENTAL PROCEDURE AND RESULTS

Experimental Animals

Ten male rhesus monkeys (macaca mulatta), approximately seven years old were used for this study. The animals were radiographed to ensure that there were no congenital, or acquired postural abnormalities in their musculoskeletal structure. Selection of a subject was difficult, but the rhesus monkey was selected for several reasons. First, they are considered to be an excellent model for bone remodelling research (Mack et al. 1967, Swenson 1987, and Kazarian and von Gierke 1971). The growth and development, as well as overall geometry and architecture of the skeletal system correlates well with the human skeletal system (Beddoe 1978 and France 1984). In many cases bone strength, fracture healing patterns, and disuse-related bone degeneration compare closely with human clinical findings (Mack 1967, and Kazarian and von Gierke 1969). Secondly, in contrast to lower animals such as rodents, the rhesus skeletal response to stress involves bone remodelling as well as modelling. Small mammals undergo remodelling to a limited extent which is confined to specific areas of bone and displays an irregular activity. (Hert 1972)

Other lower animals, such as the pig would not provide a good model due to the variances in bone density. "Clearly the trabecular structure of the human bones are very much less compact than those of the beagle and miniature pig, while the rhesus monkey bones are in this respect more similar to the human bones than to those of other animals." (Beddoe 1978) Mean trabecular path length and percentage bone volume were much greater for the miniature pig

and surface-to-volume ratios in the pig were much smaller, albeit varying little between other species. (Beddoe 1978) Bone density is a critical parameter between species when observing effects of radiation, and the bone density of the rhesus monkey parallels that of the human (Pope et al. 1989). Density will affect the linear attenuation of the photons which in turn will critically affect the absorbed dose. In this study it is important that the absorbed dose of the animal subjects be as close as possible to that which would be observed in humans, in order to make valid comparisons. Finally, anthropomorphically a biped is preferred for bone remodelling studies of the vertebral column, as the skeletal loading mechanism is more similar to that of a human.

Animal identification numbers, beginning weights, ages and treatment group are presented in Table 1. The animal's treatment group was randomly selected using a random number generator. The animals were housed as they existed in the Aerospace Medical Research Laboratory Veterinary Sciences Building, Wright-Patterson Air Force Base. The animals were fed a diet of approximately 10 monkey chow biscuits (Purina Monkey Chow) twice per day, and half an apple once per day. On days when labeling or the radiation exposure were accomplished, the animals were not fed in the morning prior to the treatment. This was necessary when any type of anesthetic was used, so that the animal would not asphyxiate on ingested food.

In Vivo Samples, Measurements and Administration

Below is a list and description of samples and tissues collected before necropsy.

1. Blood serum-Approximately 5 ccs of blood was collected via the femoral artery. Blood was collected in the mornings the week prior to the radiation treatment, each week for three weeks after and every two weeks until necropsy. This was placed in EDTA treated tubes for routine hematological analysis. The blood analysis was to

TABLE 1

SUBJECT IDENTIFICATION, BIRTH DATES, WEIGHTS AND TREATMENT GROUP

SUBJECT	BIRTHDATE	WEIGHT(kg)	TREATMENT GROUP
JU	4/8/81	9.6	IRRADIATED
N610	3/24/81	8.6	IRRADIATED
N620	4/?/81	11.8	CONTROL
N626	4/23/81	8.8	IRRADIATED
N630	4/29/81	9.8	IRRADIATED
N639	5/5/81	9.4	CONTROL
N656	5/26/81	13.6	CONTROL
N669	6/12/81	10.6	IRRADIATED
N680	6/25/81	9.6	IRRADIATED
N685	7/11/81	10.8	IRRADIATED

ensure that the animals remained healthy following the radiation therapy treatment.

2. Radiographs-Lateral view and anterior-posterior view radiographs were taken prior to selecting the animals for the study and just prior to necropsy to allow for density measurements.

3. Health Records-Records of experimental procedures performed, food intake and animal health were kept routinely during the course of the experiment.

4. Bone labeling-Osteochromes (bone labels) were given at four different times: twice before irradiation and twice just prior to necropsy.

Necropsy and Tissue Collection

Necropsies of the animals occurred on two consecutive days 105 days following the radiation treatment which occurred on two consecutive days. The tissue used for biomechanical tests was prepared by separating the vertebral bodies, removing all the soft tissue and intervertebral discs, and by removing all processes including the lateral, and posterior processes. These were frozen until further preparation was completed. The vertebral bodies used for histomorphometry were placed in 70% ethanol until further preparation could be completed. It was observed in the pathology report that two of the animal subjects had predominately fatty replacement of bone marrow tissue in vertebrae other than those analyzed for this study. This has been commonly found in autopsies of radiation therapy patients (Schantz et al. 1971). Other tissues were collected for other studies so as to obtain a greater amount of usefull information from each animal. These included the femurs, patellas, thoracic level twelve and lumbar levels one and five.

Radiation Dose Administration and Dosimetry

Dose Administration

Seven of the ten rhesus monkeys were irradiated. The animals were preanesthetized with ketamine (15 mg/kg) followed with a mixture of halothane and nitrous oxide during radiation treatment and transport. The animal subjects were transported from the veterinary facility in transport cages to the linear accelerator in the Wright-Patterson Air Force Base Medical Center Radiation Therapy Department. (See Figure 1.) Each subject's treatment field was simulated using a Varian Ximatron CX Radiotherapy Simulator (Varian Associates, Inc., Palo Alto, CA 94303). A field of approximately 7 cm in length by 3.5 cm in width was used for the specific lumbar levels 2, 3 and 4 and also including the outer adjoining discs (between L1 and L2, and L4 and L5) to assure that all of L2, L3 and L4 were included in the radiation treatment field. (See Figure 3 and 4.) A depth of 3 cm from the skin surface to the center of the vertebrae was chosen as the treated reference depth. To treat 1300 cGy to the reference depth, calculation of the correct monitor units was completed with a Computerized Medical Systems Treatment Planning System (CMS Inc., Maryland Heights, MO 63043). The dose of 1300 cGy was administered posterior to anterior in one single exposure at a dose rate of 260 monitor units (MUs) per minute. Previous work has shown this dose to be biologically equivalent to 40 Gy delivered in a fractional regime as calculated by the following formula (Powers 1988):

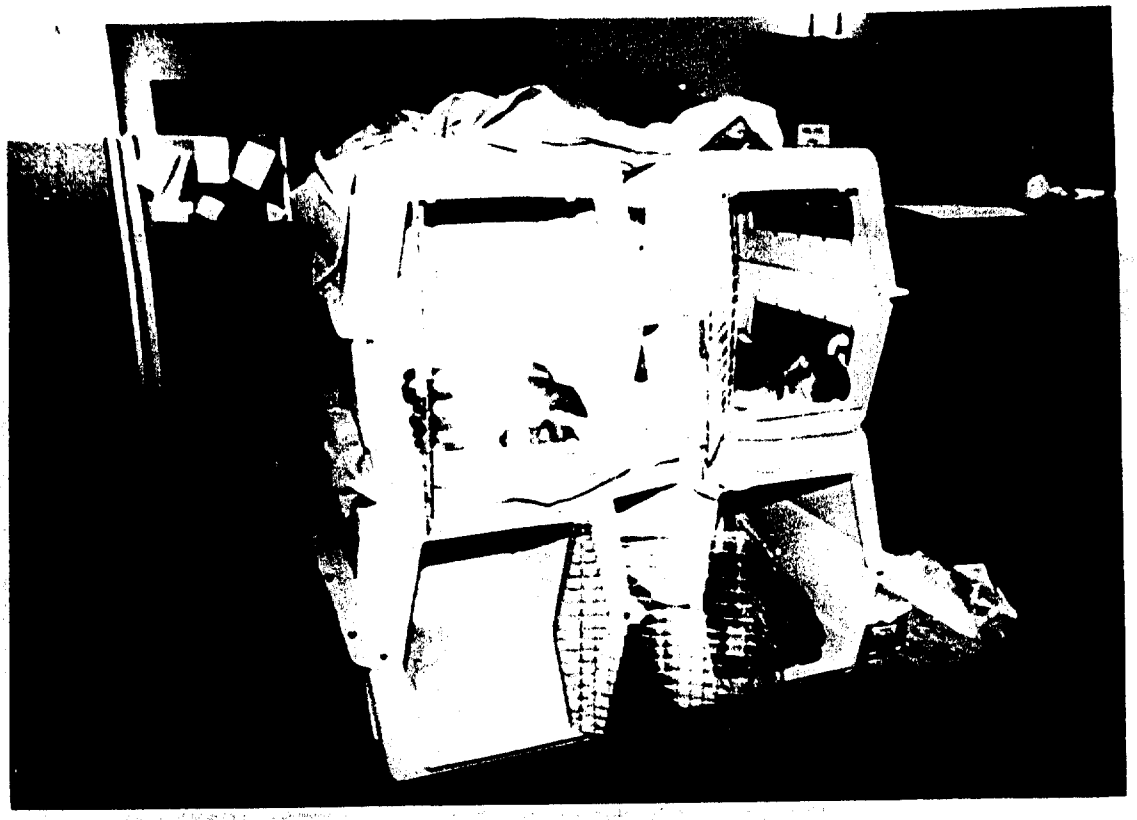

Figure 1. Transport of animals from the veterinary facility to the radiation therapy department.

Figure 2. Rhesus monkey in position in linear accelerator treatment room. The rectangle on the skin of the subject represents the treatment field.

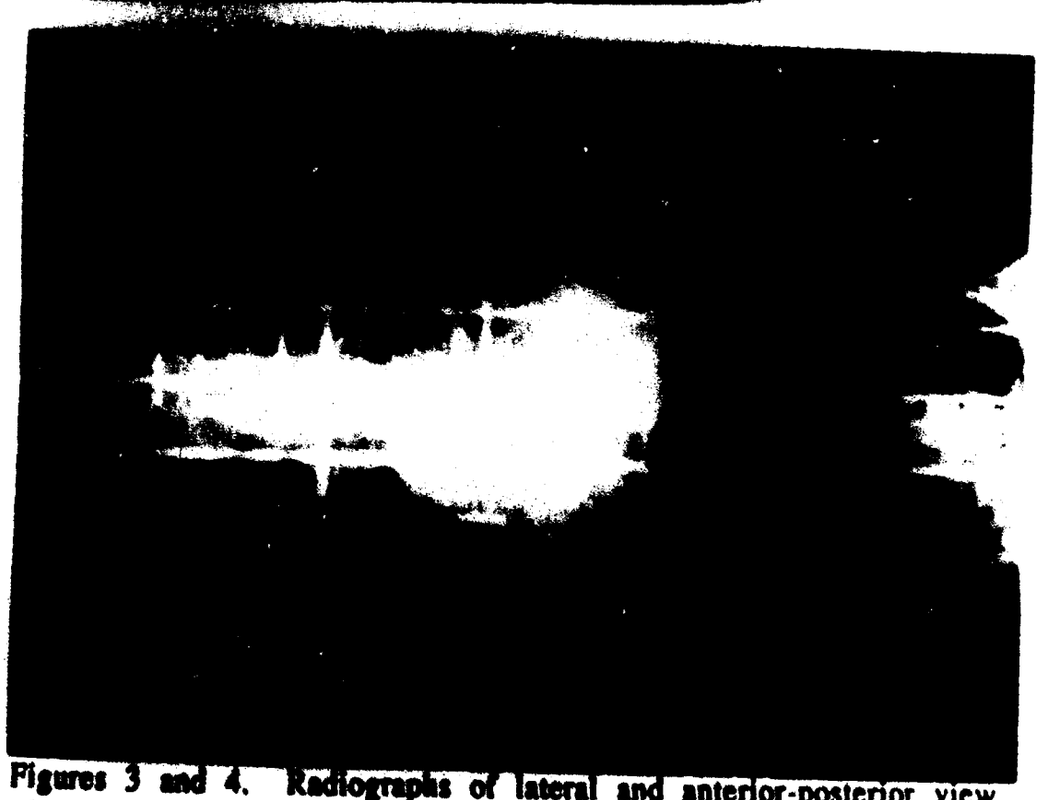

Figures 3 and 4. Radiographs of lateral and anterior-posterior view of the treatment field from the simulator set up.

$$d_{new} = \frac{a/\beta + d_{ref}}{a/\beta + d_{new}} (D_{ref})$$

where 40 Gy is the reference dose (D_{ref}) and 200 cGy per fraction is the fractionated dose (d_{ref}) and the a/ß ratio is 3, solving for d_{new} by quadratic equation the new single dose would be 12.7 Gy. (Withers 1988) The dose of 40 Gy was chosen as it is representative of a total dose given in a radiation therapy treatment. The dose was administered utilizing 6 MV (megavolts) photons from a Clinac 1800 linear accelerator (Varian Associates, Inc., Palo Alto, CA 94303) at 100 SSD (source-to-surface distance) and 260 MU pre minute. Port films were taken to verify the proper treatment field.

The animals were treated on two consecutive days. Three animals were treated the first day and four animals were treated the second day. The entire procedure took about 4 hours during which time all the animals were anesthetized. (Figure 2) Two of the seven animals went into shock following the treatment. This was thought to be due to the extensive time duration that the animals were under anesthetic and possibly, the bone labeling compounds interfered with the ability of the liver to metabolize the anesthetic. The animals were hypothermic, therefore warm IV fluids were given while increasing the animals body temperature with warm water enemas and warm baths. The two animals recovered and were thereafter asymptomatic. The control animals were not anesthetized.

Dosimetry

It was critical to this study to assure that the proper dose was administered to the three lumbar vertebral bodies in study and to assess the scatter to the adjacent vertebrae. There may be as much as a 500 cGy gradient from the posterior to the anterior margins of the vertebral bodies and the dose may be different for each particular vertebral body (Parker and Berry 1976). Iso-dose curves were computed using a CMS Treatment Planning System with the results shown in Figures 5 and 6. The density of a bone used for

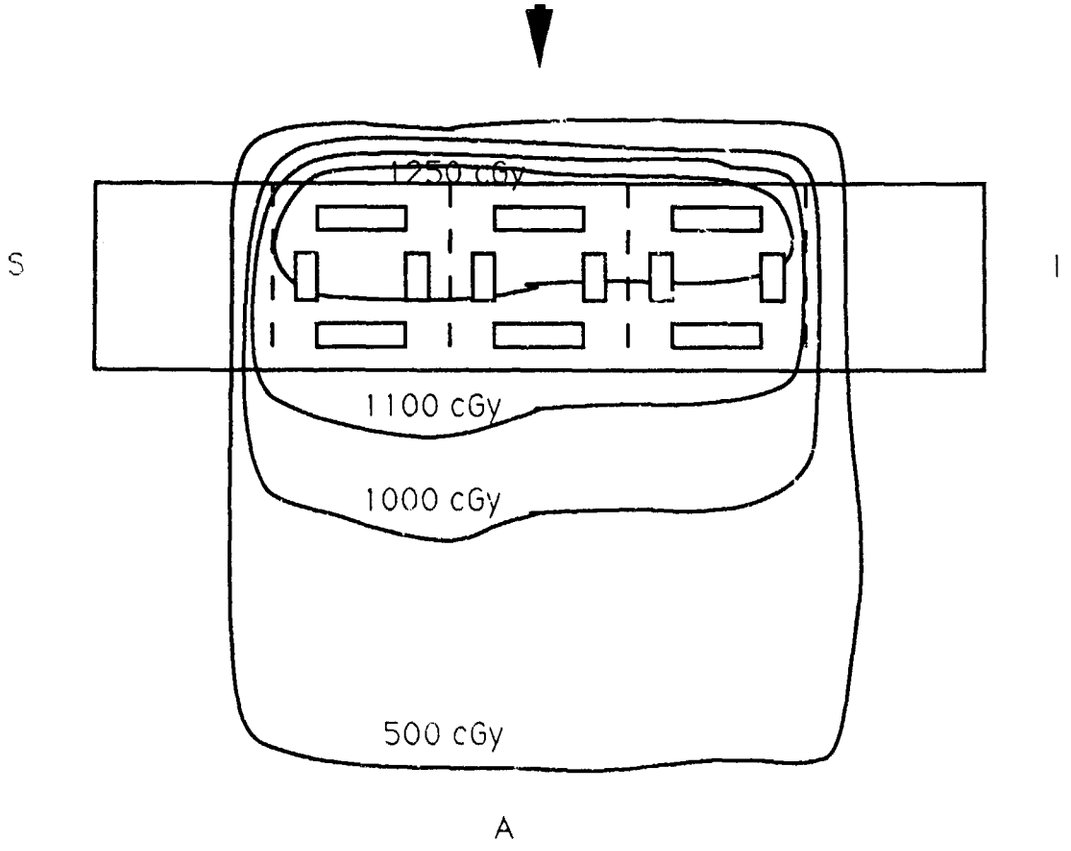

Figure 5. Isodose curves calculated from the treatment plan showing sagittal view of lumbar spine. Dashed lines represent the division of the five lumbar vertebrae. The direction of the photon beam is represented by an arrow. Orientation of spine denoted with S (superior), I (inferior), and A (anterior). Relative positions of the histomorphometry regions are indicated by rectangles.

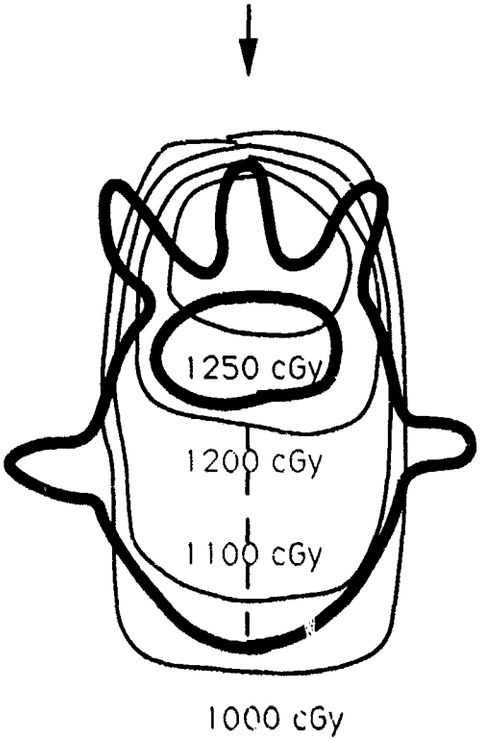

Figure 6. Isodose curves calculated from the treatment plan showing superior view of posterior to anterior directed irradiation. Direction of photon beam is indicated by an arrow. Relative position of the histomorphometry regions is indicated by the dashed line

calculation was 1.2 gm/cc (ICRU Report 24, 1976 and Sontag and Cunningham, 1977). All other tissue was considered 1 gm/cc. In addition to the treatment dosimetry plan, thermoluminescent dosimetry calculations were also used.

Seventy-four lithium fluoride thermoluminescent dosimeters (TLDs) were selected from 120 batched TLDs. Selection was done after annealing all TLDs at 400 degrees Celsius for one hour, and then 24 hours at room temperature using a Box Type Muffle Furnace, (Blue M Electric Company, Blue Island, IL 60406, Model E-514A-1). The TLDs were then irradiated to 1500 cGy at a dose rate of 260 monitor units per minute at d_{max} (1.5 cm for 6 MV photons) utilizing a 6 MV photon energy. Readings of the TLDs were completed using an Automated TL Analyzer System (Model 2000D), and Automatic Integrating Picoammeter (Model 2000-B, The Harshaw Chemical Company, Solon OH 44139), and a Digital Recorder (Model 6110, United Systems Corp., Dayton OH 45403). The TLD readings were ranked in numerical order and the lowest and highest values were eliminated leaving the center 74 TLD readings. Each highest reading TLD and the lowest reading TLD were paired until the remaining center two TLDs were paired. The TLDs were again annealed at 400 degrees Celsius for one hour and then 24 hours at room temperature.

A calibration curve was created using 24 of these TLDs. Six sets of 4 TLDs each were irradiated at d_{max} at six different doses: 300, 500, 800, 1000, 1500, and 2000 cGy. The response curve is shown in Figure 7. Calculation of TLD readings were made from this curve. (Horowitz 1984)

Each pair of TLDs were wrapped in cellophane wrap then aligned between two pieces of hypoallergenic cloth tape in a row of five pairs. This strip was then placed along a rhesus monkey cadaver spine as in Figure 8. The spine from a 9 kg, six year old rhesus monkey was used for the dosimetry analysis. (Procured from Yerkes Primate Research Laboratory, Emory University, Atlanta GA.) Five strips were prepared. One for the anterior of the spine, two for each lateral anterior aspect of the spine and two for each side of the spinous process. The entire spine was then wrapped in cellophane

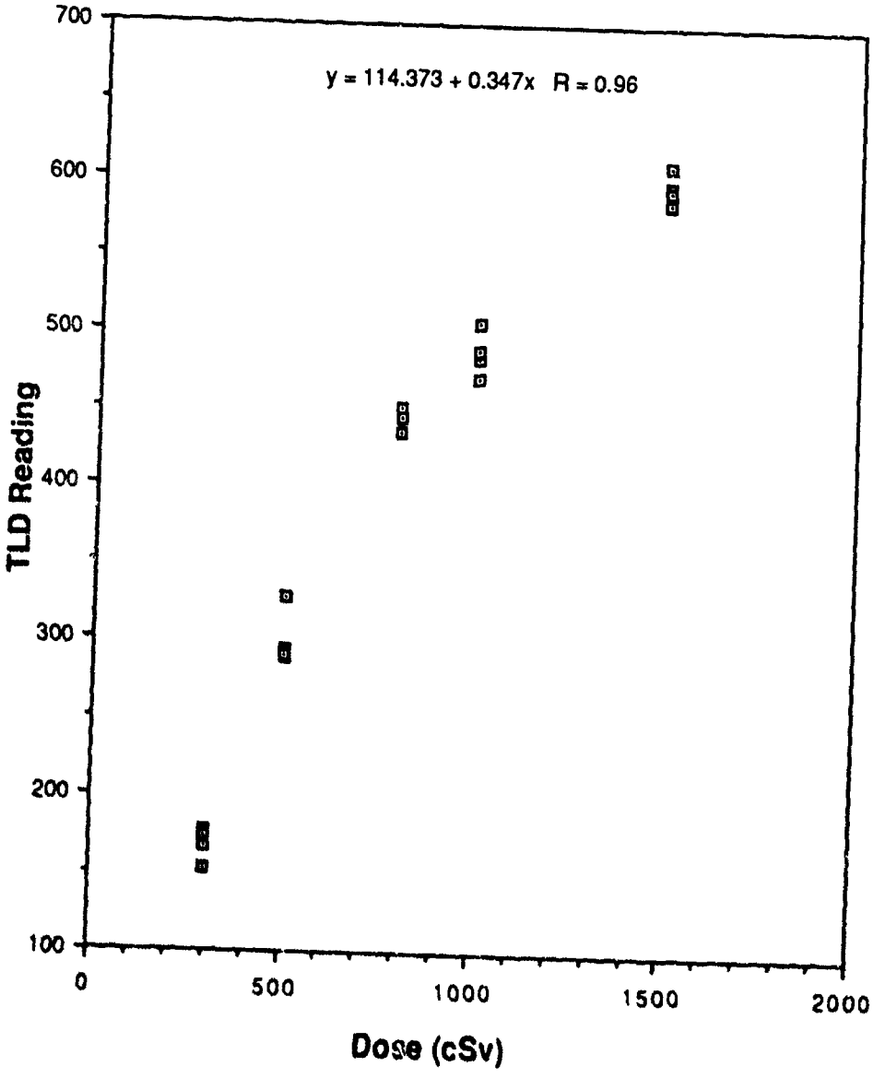

Figure 7. Calibration curve of lithium-fluoride thermoluminescent dosimeters

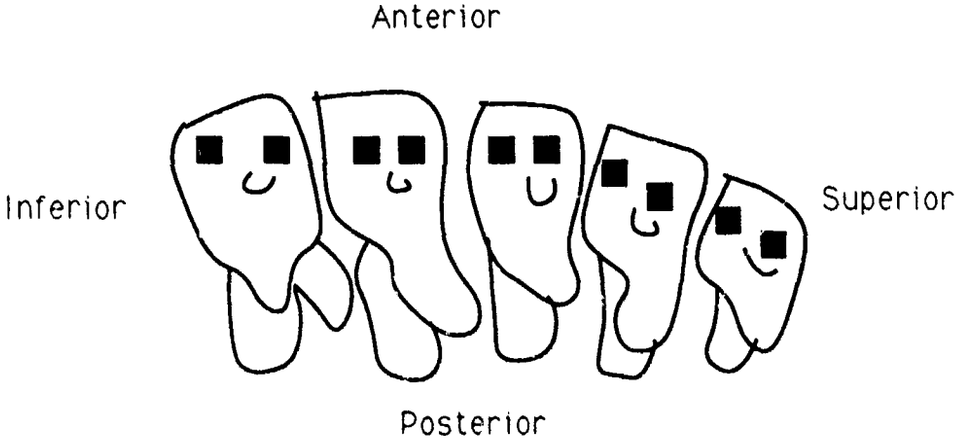

Figure 8. Placement of the thermoluminescent dosimeters on the left anterior portion of the vertebrae. Each pair of dosimeters were wrapped in celophane wrap , placed between two strips of hypoallergenic cloth tape and placed along the vertebrae.

wrap and placed in a vacuum sealed plastic bag and again in a second sealed plastic bag. A tub of 12 cm of water was used to simulate tissue for backscatter with the posterior process of the spine submerged 0.5 cm under the water's surface. A dose of 1300 cGy was delivered to a reference depth of 3 cm with a field of 3.5 cm in width and 7 cm in length. The TLDs were then removed from the cellophane wrap and read using the Harshaw Analyzer System.

Results

The treatment plan in Figures 5 and 6 demonstrate that there was a dose gradient of 150 cGy from the posterior to the anterior spine. The posterior dose was about 1250 cGy with the rest of the spine including the anterior portion receiving 1100 cGy. The adjoining lumbar vertebra (L1 and L5) received approximately 500 cGy at the location where they join L2 and L4 as shown in Figure 5.

When the wrapping was taken off the rhesus monkey cadaver spine following the dose for the TLD analysis, it was evident that the anterior strip of TLD had become misaligned, with the TLDs on lumbar one and lumbar two off center. The other three pairs of TLDs on lumbar levels L3, L4 and L5 were in the correct position. The doses to the anterior location of L3 and L4 were 738 cGy and 898 cGy respectively. The right anterior strip of L2, L3 and L4 received doses between 145 cGy and 869 cGy. The left anterior strip received between 1060 to 1089 cGy. This discrepancy, or off balance, would seem to indicate that the spine was slightly misaligned and the dose that was delivered to the right lateral side traveled through more of the processes, which are primarily cortical bone and therefore more dense, thus resulting in a lower dose. A slight misalignment could account for a dose gradient if this were the case. The lateral strips varied form 834 cGy (right lateral) to 1080 cGy (left lateral). These dose variations are displayed in Figure 9.

The TLD readings on the adjacent vertebrae of L1 and L5 show a varied response from 0 cGy (unreadable value off the calibration curve) on L5 to 1077 cGy on L1. The left lateral and left anterior

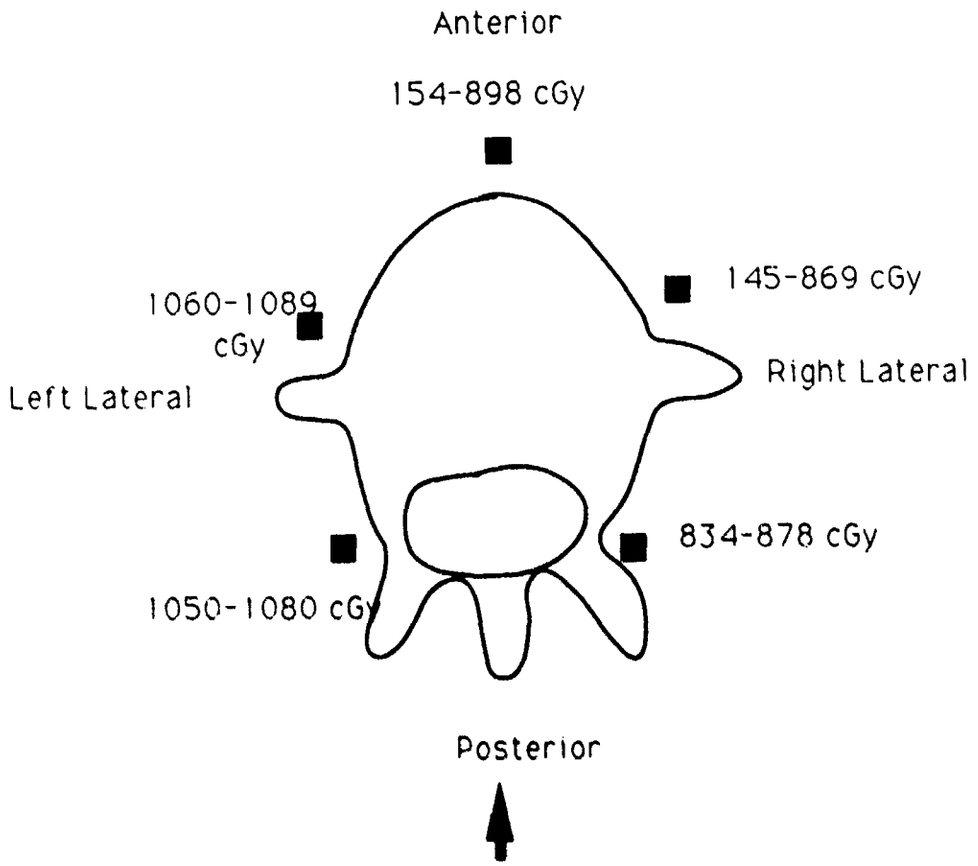

Figure 9 Placement of thermoluminescent dosimeters on vertebral bodies with superior view dose distribution for lumbar levels 2, 3, and 4 Arrow represents direction of photon beam

TLDs appeared to be in the direct field with their TLD readings of 912 cGy and 1077 cGy, respectively. The right lateral TLD reading of 309 cGy on L1 was more likely to be scatter as were the readings of 77 cGy and 95 cGy on the anterior and right anterior TLD strip. The results suggest a gradient of as much as 550 cGy :1300 cGy (given dose) minus 738 cGy (lowest viable anterior reading). The adjacent lumbar levels of one and five received approximate dose levels of 300 cGy from scatter.

Blood Analysis

Complete blood analysis was completed on blood collected from the subjects on nine different occasions: the week prior to the radiation treatment, each week for three weeks after and every two weeks until necropsy. Approximately five cubic centimeters of blood were drawn and placed in EDTA treated tubes to prevent clotting. Fourteen different routine analyses plus differential counts were completed on each sample. These included white blood cell count, red blood cell count, hemoglobin, hematocrit, mean corpuscular volume, mean corpuscular hemoglobin, mean corpuscular hemoglobin concentration, neutrophil, bands (precursors to mature white blood cells), lymphocyte, monocyte, eosinophils and platelet counts. This analysis was done primarily to assure that the animals were in good health and that the radiation did not affect them adversely. This was not expected, as the radiation was directed to a localized position and it would be unlikely that there would be any significant of the hematopoietic radiation syndrome. However, it has been observed that localized radiation can cause generalized skeletal repsonses, such as hematopoiesis (Werts et al. 1977; and Maeda et al. 1988).

Results

The animals remained in good health following the radiation treatment. There were no observed hematopoietic effects due to the radiation treatment. The reference values used for rhesus monkeys blood counts are included in Appendix 1.

Biomechanical Testing

Vertebral centra compression tests were completed on lumbar levels L2 and L3 to identify any changes in bone material strength characteristics due to the irradiation. The compression tests were performed axially to observe the ability of the bone to resist crushing. The vertebral bodies were prepared for testing by eliminating all surrounding soft tissue including muscle, ligaments and all intervertebral disc material. The processes were removed, including the lateral processes and the posterior process at the base of the pedicle. The prepared specimens were frozen in sealed plastic bags for one month before testing. Anterior and posterior heights were measured to the nearest 0.01 cm with a digital caliper and the average of these measurements was used as the original height. Magnified photographs (2X) of the superior and inferior bony end surface were taken with a camera. Area calculations of each end were done with a drawing tablet and computer system. (Zeiss Videoplan II Analysis System, Carl Zeiss Inc., Thornwood, NY). Polymethylmethacrylate (Perfex Repair Resin, International Dental Products, Inc., NY,NY) was used to fabricate thin pots to stabalize both the superior and inferior surfaces of the vertebral centrum. This ensured a parallel transmission of the load across the entire bony surface and prevent slippage between the bony endplate and the metal surface of the compression load cell. The compression testing technique employed by Kazarian (Kazarian and Kaleps, 1979; and Kazarian and von Gierke, 1981) was used. The compression tests were performed with an MTS Universal Testing System (MTS

Systems Corporation, Minneapolis, MN) equipped with a 100 KN load frame (Model 312.21) and a 25 KN universal load cell (Model 661.214-01). Figure 10 shows the MTS set up with the vertebral centrum in place between the polymethylmethacrylate pots and the MTS load cell. Data was collected via a PDP 11-34 computer in the form of load vs. displacement. The vertebral centra were compressed to 50% of their original height at a load rate of 210 in/min. The raw data from each test combined with height and average load area (calculated from end surface photographs) was reduced to provide load displacement curves and values for engineering strength parameters. The following is a list and description of the parameters determined from the compression tests as shown in Figure 11.

1. Modulus of elasticity - is the value of the stress strain ratio. It is represented as the slope on the stress-strain curve. The stiffer a material is, the higher the value of the modulus of elasticity and the more difficult it is to deform.

2. Yield stress - is the stress or force per unit area at the point where the stress-strain ratio is no longer linear, a marked increase in deformation occurs with respect to load, and plastic deformation begins to occur.

3. Yield strain - is the value of the strain or amount of deformation divided by the original length at the yield point(a dimensionless parameter).

4. Ultimate stress - is the force per unit area of load value at the point of failure or the point when the material cannot recover.

5. Ultimate strain - is the value of the strain at the point of failure.

6. Stiffness - deals with the concomitant linear increase in deformation with increasing load in the elastic region (until the yield point).

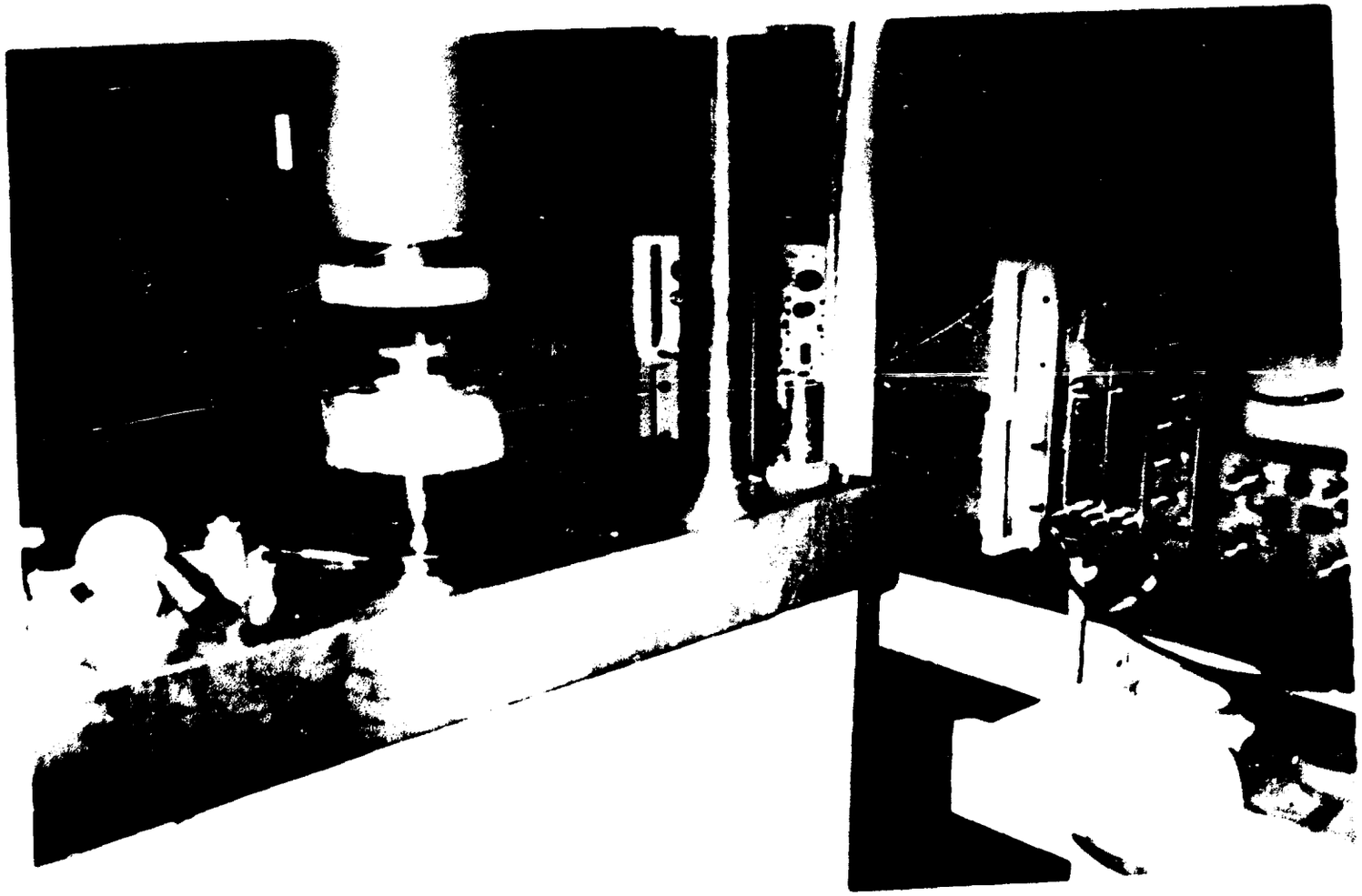

Figure 10. Material Testing System used for vertebral centrum compression test with test specimen in place with polymethylmethacrylate pots.

VERTEBRAL CENTRUM COMPRESSION TESTS

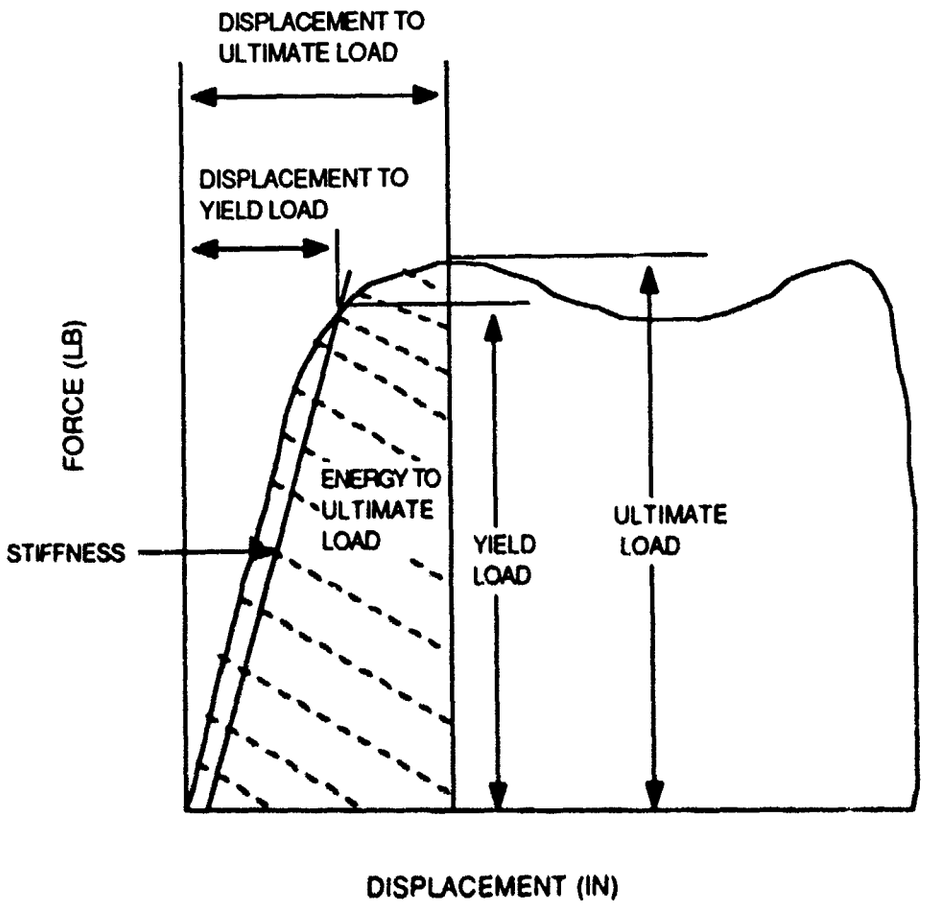

FIGURE 11. Typical load test on a vertebral centrum showing the method used to determine compressive strength parameters from force/displacement curves.

7. Yield load - is the load value at the yield point.

8. Displacement to yield load - is the amount of deformation that occurs to the yield point.

9. Ultimate load - is the load value where failure occurs.

10. Displacement to ultimate load - is the amount of deformation that occurs up to failure.

11. Energy to ultimate load - or toughness, is the amount of energy expended to produce the failure, or the area under the curve.

Five of these parameters are derived from the remaining parameters. The equations for calculating these parameters are:

Modulus = (Stiffness * H)/A
Yield Stress = Yield Load/A
Yield Strain = Displacement to Yield Load/H
Ultimate Stress = Ultimate Load/A
Ultimate Strain = Displacement to Ultimate Load /H

where H equals the average of the posterior and anterior heights of the pretest centrum and A equals the average of the superior and inferior surface pretest area.

Results

A two-factor analysis of variance was computed to test statistical significance of the compression test results. Variation between lumbar levels of L2 and L3 were calculated as well as variation between treatment groups. The numerical results are tabulated in Table 2. The means, standard deviations and sample numbers were computed for the combined lumbar levels L2 and L3 as no difference was observed between the two. Combining data for adjoining vertebrae may be done to aid in data reduction (France 1984). The P-values listed are derived from the analysis of variance calculation for between treatment group variation. As noted, no

TABLE 2

VERTEBRAL CENTRUM COMPRESSION TEST RESULTS, MEAN (X), STANDARD DEVIATION (S), AND SAMPLE NUMBER (N)

	IRRADIATED			CONTROL			P-VALUE
PARAMETERS	X	S	N	X	S	N	
Modulus of Elasticity lb/sq in	72278.143	16956.083	14	60428.333	16030.04	6	0.1879
Yield Stress lb/ sq in	3107.282	632.574	14	3098.42	649.706	6	0.9789
Yield Strain in/in	0.079	0.018	14	0.089	0.019	6	0.3179
Ultimate Stress lb/sq in	3694.944	571.866	14	3991.827	301.313	6	0.2641
Ultimate Strain in/in	0.187	0.077	14	0.217	0.081	6	0.4744
Stiffness lb/in	33447.786	8598.12	14	29789.333	8214.743	6	0.4153
Yield Load lb	1061.214	199.754	14	1043	304.05	6	0.8803
Displacement to Yield Load in	0.059	0.014	14	0.06	0.014	6	0.9315
Ultimate Load lb	1264.929	180.105	14	1321.542	122.9	6	0.5121
Displacement to Ultimate Lo in	0.14	0.062	14	0.144	0.053	6	0.9028
Energy to Ultimate Load	130.213	74.403	14	126.937	50.005	6	0.9273

statistically significant changes were observed in any of the vertebral centrum compression strength parameters. ($p \leq 0.05$)

Histomorphometry

Histomorphometry, or the quantitative study of tissues in association with bone labeling techniques, can give information about growth and modelling or remodelling in the skeletal system. Static growth parameters can be determined with any tissue samples, but use of a bone labeling compound is necessary to measure dynamic parameters. (Recker 1983; and Frost 1973, 1981)

Tetracycline HCl, xylenol orange and DCAF, used as bone labeling compounds and administered intravenously, are taken up by the "active" bone. "Active" bone is bone that is being laid down or formed during the time of high serum label concentration. The label is incorporated into the forming bone and will remain in situ until resorption occurs at some later time. A special property of these labels is that they fluoresce when a tissue section is viewed under ultraviolet light (wavelength = 400-440 nm). A labeling pattern is produced by the administration of a bone labeling compound, followed by a period of time without label (5-14 days optimum), and then another day of label administration, followed by another period without label prior to tissue collection. A typical sequence would be denoted 1,14,1:14; of which 14 days represents the period of time between doses of label and before tissue collection (Frost, 1983). Growth rate is determined by the amount of tissue measured between labels as a function of time. The following labeling compounds were used:

1) Tetracycline hydrochloride, 15 mg/kg

2) Xylenol orange, 1 ml/lb body weight in a stock solution containing 5% xylenol orange in saline

3) Dicarbomethylaminomethyl fluorescein (DCAF), 30 mg/kg body weight in a stock solution of saline containing 2% sodium bicarbonate.

4) Tetracycline was again used as the fourth label.

These labels were administered by intravenous injection 21 days prior (tetracycline) to irradiation and 7 days prior (xylenol orange) to irradiation. The two final labels were administered 21 days (DCAF) and 7 days (tetracycline) prior to necropsy. All ten animal subjects were given the bone labeling agents.

The L4 vertebral body was placed in 70% ethanol overnight followed by two new changes of 100% ethanol for a 24 hour period each. Next, the vertebral bodies were placed in half methyl methacrylate monomer (Fisher Scientific, Cincinnati, OH) and half 100% ethanol overnight at room temperature. During the following two 24 hour periods, the sections were placed in a monomer solution (consisting of 1 gm benzol peroxide and 100 ml methyl methacrylate monomer) and refrigerated (35-40 F). The thin monomer was then replaced by a thick monomer, consisting of 2 gm benzol peroxide, 100 ml methyl methacrylate monomer, and 40 gm polymethylmethacrylate beads (Fisher Scientific, Cincinnati, OH) and mixed to the consistency of honey and refrigerated overnight. Finally, a new solution of thick monomer replaced the old one and the specimen was left for 3 days in a vacuum. The vacuum removed air bubbles and the specimen was then embedded in hardened plastic material. See Figure 12. A Reichert-Jung Polycut bone saw (Model E, Heidelberg, West Germany) was used to plane off the embedded vertebrae. (See Figure 13.) Once the embedded vertebrae was faced to the desired sectioning level, a length of rubber resin adhesive (3M Company, St. Paul, MN) was applied to the block face and all air bubbles were removed by smoothing the tape down with a finger. As the bone saw begun to cut, the edge of the tape was held so that the 10 micron section would be removed with the tape. This procedure reduced shattering, damaging and distortion of the mineralized tissue section (Hardt 1986). Four contiguous midsagittal sections from each animal were then stained

Figure 12. Lumbar 4 vertebrae embedded in polymethylmethacrylate and cut in half in preparation of thin slicing on precision bone saw.

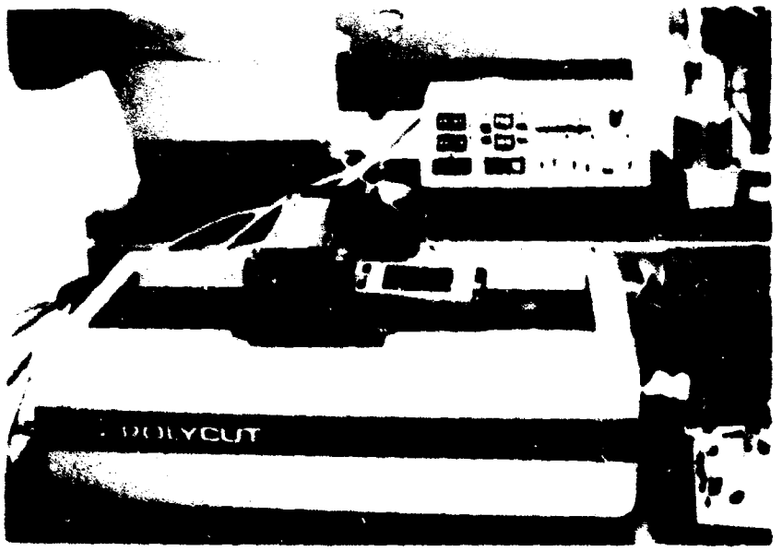

Figure 13. Polycut precision bone saw for cutting the embedded vertebral sections to 10 micron thick slices.

with mineralized bone stain (MIBS, Poly Scientific, Bay Shore, NY 11706) for 48 hours. The sections were rinsed in tap water, distilled water, and then differentiated in 0.01% glacial acetic acid in 95% methanol for 30 minutes. Finally, the sections were dehydrated in 95% alcohol for an additional 15 minutes. (Villaneueva 1989) Mounting on glass was accomplished with Euparal mounting medium (Roboz Surgical Instruments Co., Inc., Washington, DC). (See Figure 14.) One additional 10 micron section was not stained, but was mounted directly on a glass slide for analyzing the osteochrome labeling, as the bone labeling washes out during the staining process.

The histomorphometric analysis was accomplished with a Zeiss Photomicroscope I equipped with an HBO-50 watt Mercury Illuminator for reflected and transmitted light (Carl Zeiss Inc., Thornwood, NY) as shown in Figure 15. Magnification for all measurements was 100X. Histomorphometry was performed on four midsagittal trabecular bone sections from each lumbar vertebral body collected. Four separate trabecular bone histomorphometric analysis sites were chosen for the lumbar 4 bone sections. (See Figure 16.) In each of these four regions, sixteen microscopic fields were used. A microscope field was 0.790 mm in width by 0.790 mm in length and 0.624 mm^2 in area as shown in Figure 17. Each region was divided into sixteen fields or eight fields in length by 2 fields in height for a total regional analysis area of 9.986 mm^2. The location of the superior region was determined by finding the lower most portion of the superior bony endplate and moving down two full fields. The eight field wide region was then centered between the anterior and posterior edge. The inferior area was located in much the same manner. Similarly, the anterior and posterior regions were located two fields in from each edge, and centered between the superior and inferior edge surface. Measurements were collected and stored using a Zeiss Videoplan II Analysis System. This system expedites measurements taken by making volume, area, and length determinations, etc. A digitizing tablet and an operator controlled cursor on the digitizing tablet are projected into the microscope viewing field. The operator traces around the various bony

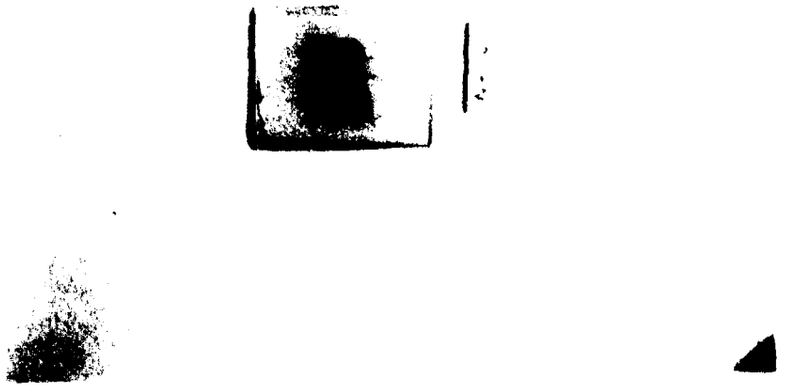

Figure 14. Lumbar four vertebral section mounted on slide.

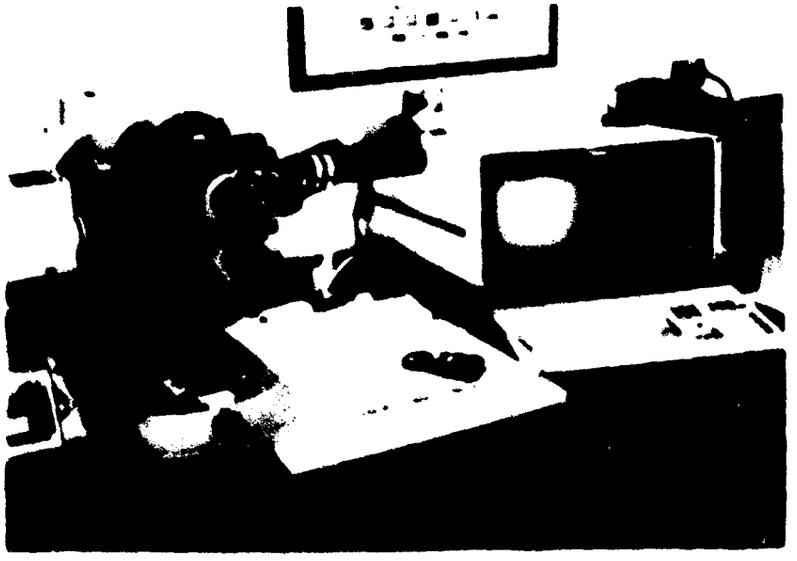

Figure 15. Zeiss photomicroscope and Videoplan computer system used for histomorphometric analysis.

MICROSCOPIC FIELD

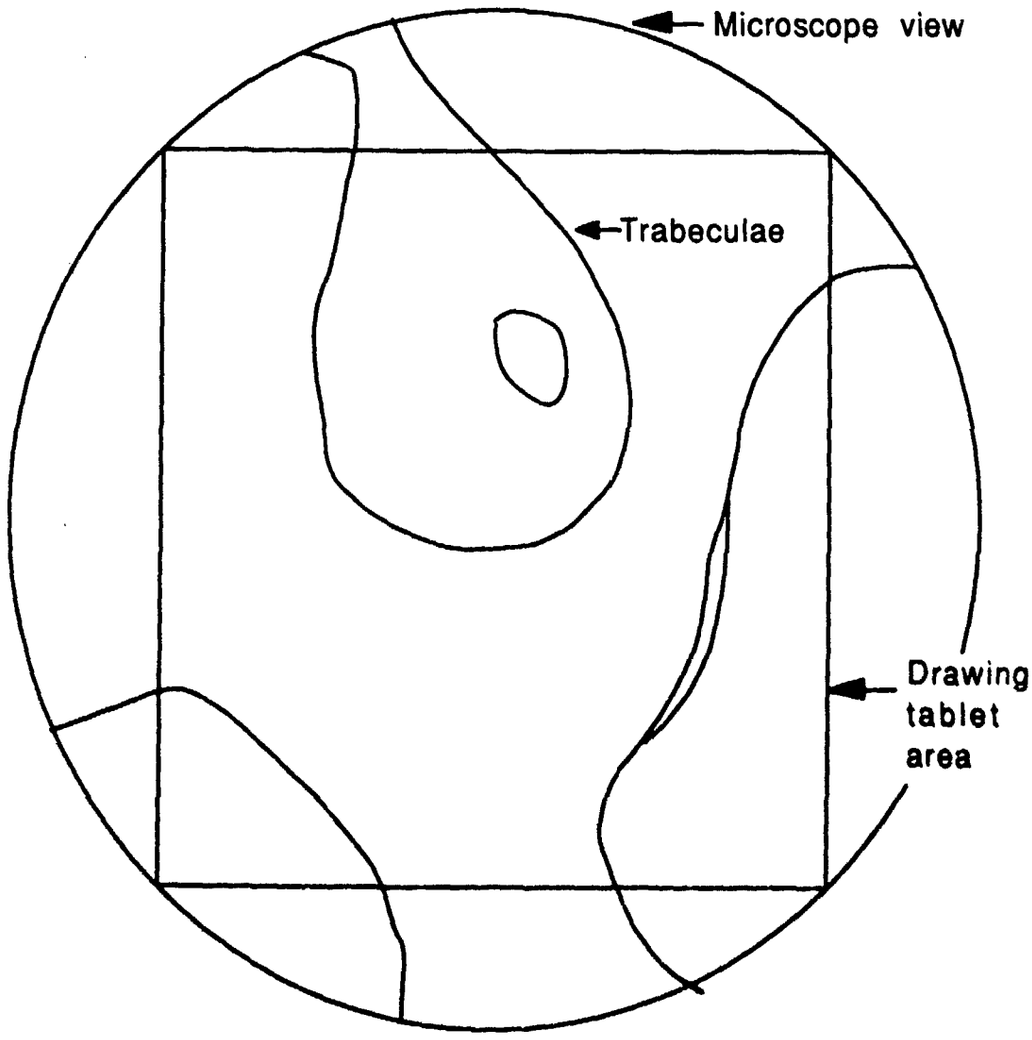

FIGURE 16. View of the microscopic measurement field. The circle is the view through the microscope. The square represents the active measurement area of the drawing tablet.

HISTOMORPHOMETRIC ANALYSIS SITES

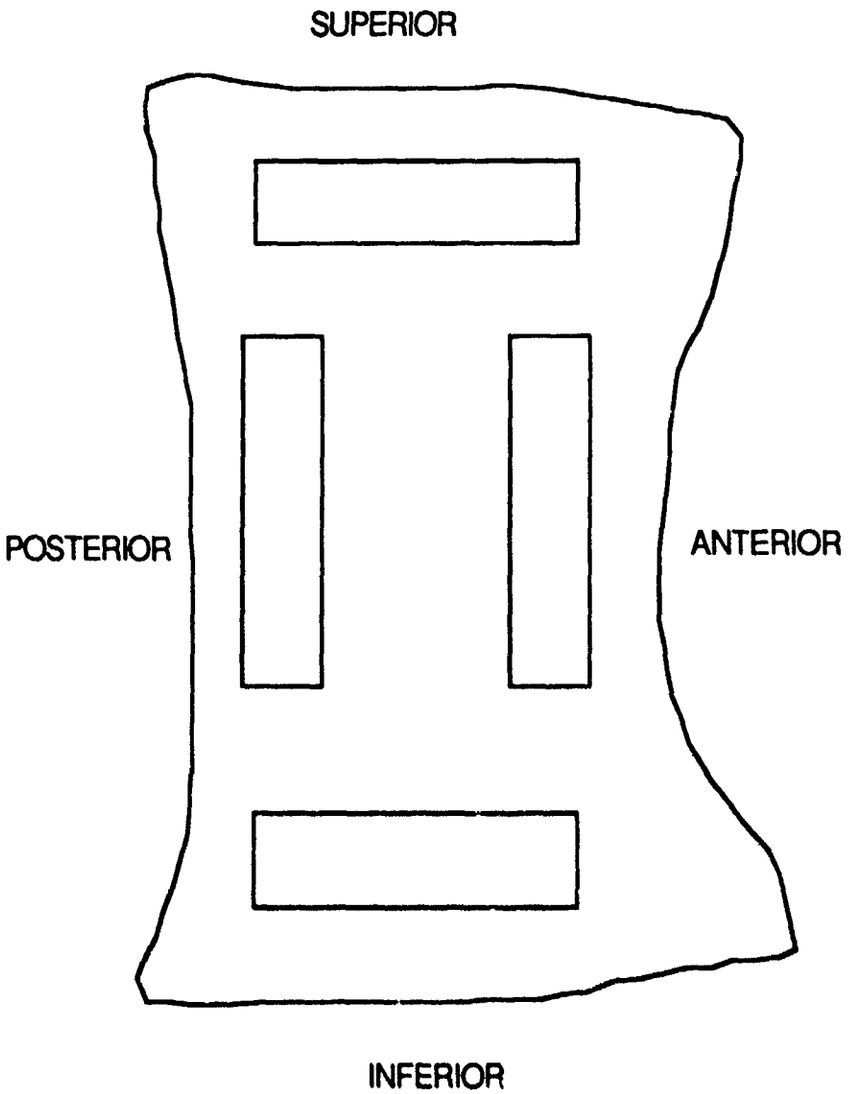

FIGURE 17. Lumbar 4 vertebral centra midsagittal sections illustrating location of histomorphometric analysis sites. Each site is designated by its anatomical location.

structures and stores these measurements into the adjoining computer. The following measurements were collected for each viewing field: (1) area of trabecular bone, mineralized and unmineralized, (2) areas of holes and empty space within the trabecular bone, (3) area of osteoid, or unmineralized bone, (4) area of resorption spaces or Howship's lacunae with osteoclasts present, and (5) mean trabecular wall thickness. Two additional measurements were collected on the unstained sections to observe the dynamic properties of the bone. These were 6) the distance between double labels (under ultraviolet light) and 7) the length of double labels (under ultraviolet light). These last two measurements were collected by using labeling data from the entire slide. While it was still divided into four regions (superior, inferior, anterior and posterior) the whole vertebrae was used to measure these two parameters. From these individual measurements, a semi-automatic stereology computer program computed volumetric density and surface volumes along with lengths and perimeters. The accumulative measurement data from all fields analyzed were converted from two-dimensional to three-dimensional values through principles of stereology (Parfitt, 1983b). Figures 18 through 21 picture examples of the desired parameters. Using this information, the following parameters were chosen as a representative array of possibly useful histomorphometric parameters. These parameters listed below are proposed by the American Society of Bone and Mineral Research to standardize the terminology used for bone histomorphometry (Parfitt 1988). Malluche's nomenclature is also included for easy transition. (Malluche et al. 1982). Also see Table 3.

1. Bone volume, (BV/TV), %, or volumetric density of bone, (VV), mm^3/cm^3, is the volume of mineralized and unmineralized bone per volume of total bone, including marrow and trabecular bone.

2. Bone surface (BS/TV), mm^2/mm^3, or bone surface density of bone, (SV), mm^2/cm^3, is the trabecular surface area per volume of total bone.

Figure 18. Trabecular pattern of bone with lining cells and osteoid which is the darkened area marked by arrows.

Figure 19. Osteoclast with multiple nuclei identified with arrows.

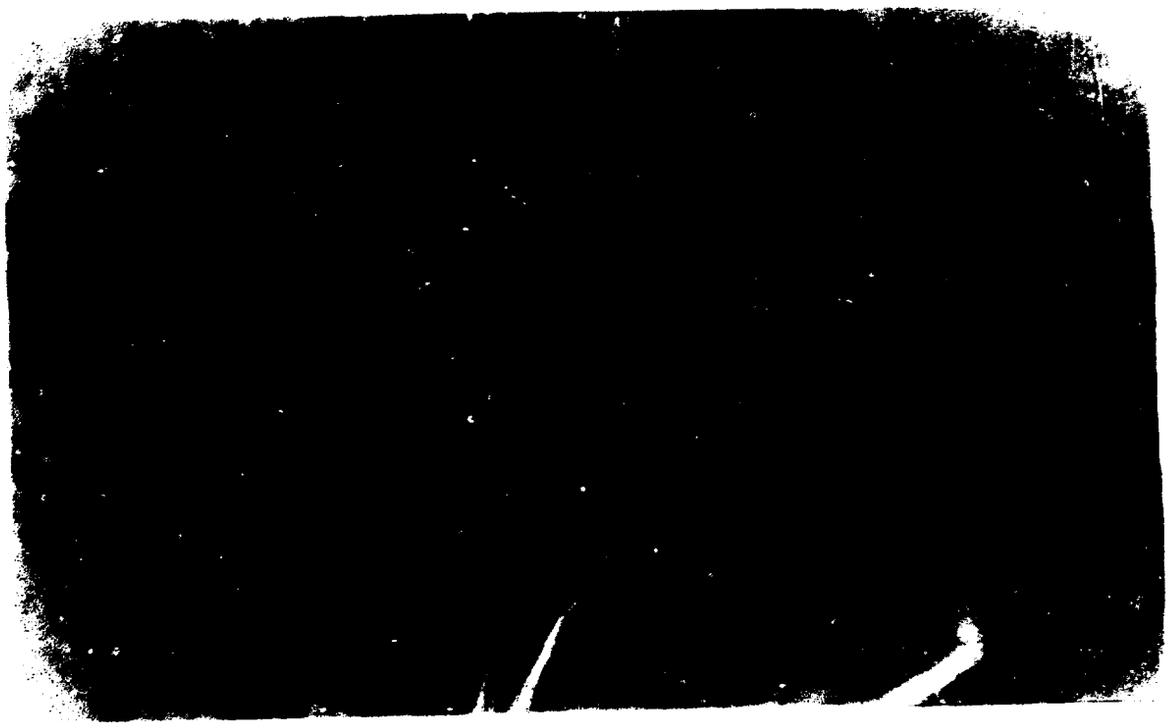

Figure 20. Osteochrome evident under ultraviolet light (100X). Two labels (tetracycline and xylenol orange) are identified by arrows.

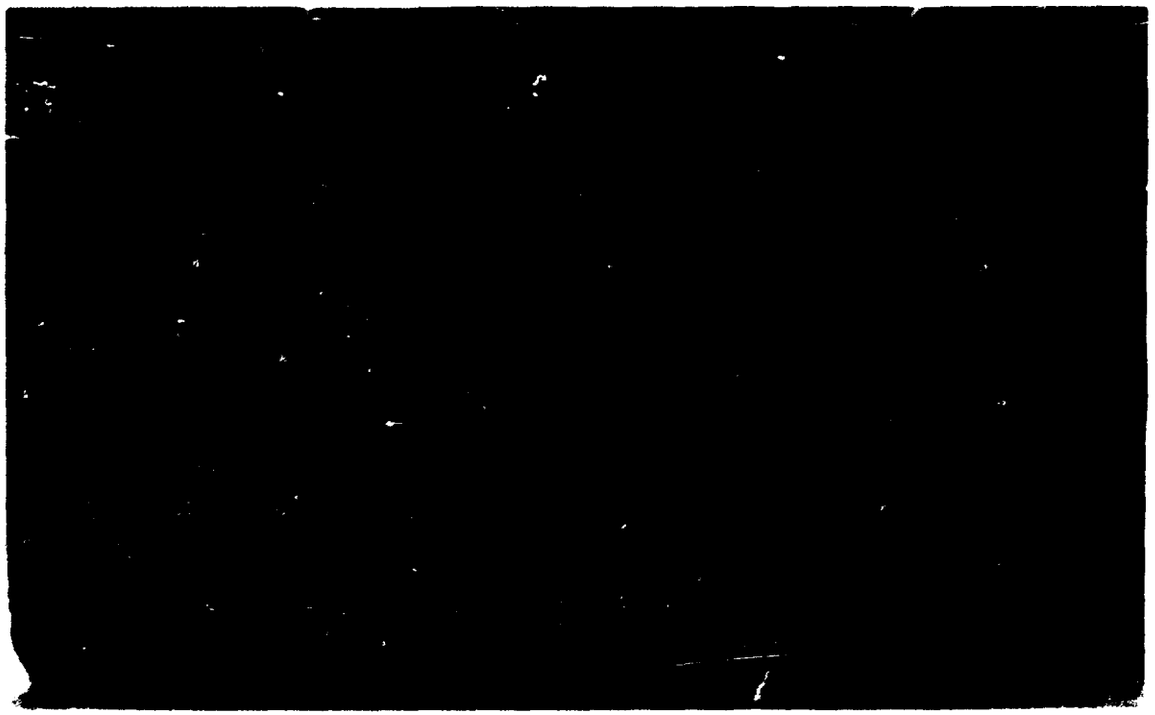

Figure 21. Osteochrome under ultraviolet light (100X) displaying all four bone labels given (tetracycline, DCAF, xylenol orange and tetracycline).

TABLE 3

VERTEBRAL CENTRUM TRABECULAR BONE HISTOMORPHOMETRIC ANALYSIS PARAMETERS

PARAMETER	ASBMR SYMBOLS	MALLUCHE'S SYMBOLS	DIMENSIONS
Bone Volume	BV/TV	VV	%
Bone Surface	BS/TV	SV	mm2/mm3
Trabecular Thickness	Tb.Th	D-trab	µm
Osteoid Volume per Bone Tissue	OV/TV	V-VOS	%
Osteoid Surface	OS/BS	%OS	%
Osteoid Volume	OV/BV	VVO	%
Osteoclast Surface	Oc.S/BS	%OR	%
Wall Thickness	W.Th	MWTH	µm
Osteoid Thickness	O.Th	TH-OS	µm
Mean Distance Between Double Label	MD-D	MD-D	µm
Fraction of Trabecular Surface Exhibiting Double Label	LAB-TS	LAB-TS	
Adjusted Appositional Rate	AjAR	AR/Y	µm/day
Bone Formation Rate	BFR/BS	BFR-TS	µm3/µm2/yr

3. Trabecular thickness, (Tb.Th), µm, or mean trabecular diameter, (D-trab), µm, is the average width of the individual trabeculae in a unit volume of bone.

4. Osteoid volume per bone tissue, (OV/TV), %, or volumetric density of lamellar osteoid, (V-VOS), mm^3/cm^3, is the volume of lamellar osteoid (unmineralized bone tissue) per unit of bone tissue.

5. Osteoid surface, (OS/BS), %, or percent of trabecular surface covered by lamellar osteoid, (%OS) represents the percent of trabecular bone surface area covered by both active and inactive osteoid. This parameter was determined by dividing the calculated SV osteoid by the surface density of bone.

6. Osteoid volume, (OV/BV), %, or the relative volumetric density of osteoid, (VVO), mm^3/cm^3, is the volume of osteoid per unit volume of trabecular bone. This parameter is determined by dividing the calculated VV of osteoid by the volumetric density of bone.

7. Osteoclast surface, (Oc.S/BS), %, or percent of trabecular surface exhibiting Howship's lacunae, (%OR), is the total trabecular bone surface covered by resorption spaces, with osteoclasts. The length of the resorption space divided by the perimeter of trabecular bone, plus the perimeter of the holes, determined this parameter.

8. Wall thickness, (W.Th.), µm, or mean wall thickness, (MWTH), µm, is the mean distance between cement lines and a completed bone surface.

9. Osteoid thickness, (O.Th), µm, is the average thickness of the unmineralized bone.

10. Mean distance between double label, (MD-D), µm, is the average distance between two labels for the analysis site.

11. Fraction of trabecular surface exhibiting double label (LAB-TS) is the fraction of trabecular bone surface overlying a double label of osteochrome. This was determined by the length of double label per the perimeter of trabeculae plus perimeter of the holes.

12. Adjusted appositional rate, (AjAR), μm/day, or appositional rate per year, (AR/Y), mm/year, is the average thickness of the layer of new mineralized bone laid down per unit of time.

AjAR = MD-D/t; where t = the number of days between the two labels

13. Bone formation rate, (BRF/BS), $\mu m^3/\mu m^2/yr$, or Malluche's bone formation rate, (BFR-TS), $mm^3/(mm^2 \times yr)$, is the volume of new mineralized bone per area of trabecular surface per unit time in years. BFR/BS = AjAR x LAB-TS x 365

Results

The results of the histomorphometry are tabulated in Tables 4 through 11. Tables 4 through 7 represent the data collected from the four stained slides from each animal for each different region: superior, inferior, anterior, and posterior. Each region of 16 microscopic fields was considered a random sample of the whole region and one sample number (N). Thus for the irradiated data there are 28 samples, those being four slides per animal times seven animals, and similarly for the control. A two way analysis of variance was used as the statistical means to either reject or not reject the null hypothesis. In eight parameters the null hypothesis was rejected which stated that the means between the treatment groups were equal. These parameters were bone volume, bone surface, osteoid surface, osteoid volume per bone tissue, osteoid volume, bone formation rate, fraction of trabecular surface exhibiting double label, and wall thickness. In these eight cases, Scheffe's t-test was used to determine which pairs of means were different.

In Tables 4 through 7, it is indicated which parameter had significant finding from the Scheffe's t-test. An asterisk indicates a significance level of $p \leq 0.05$ between treatment and control. Bone

TABLE 4

BONE HISTOMORPHOMETRY, LUMBAR FOUR ANALYSIS, SUPERIOR REGION, MEAN (X), STANDARD DEVIATION (S), AND SAMPLE NUMBER (N)

	IRRADIATED			CONTROL			
PARAMETER	X	S	N	X	S	N	
BV/TV %	23.606	4.313	28	27.175	5.263	12	*
BS/TV mm2/mm3	5.685	0.878	28	6.103	1.158	12	
Tb-Th µm	0.416	0.05	28	0.469	0.054	12	
OV/TV %	0.494	0.331	26	0.55	1.1	9	
OS/BS %	20.888	12.316	26	6.956	6.619	9	*
OV/BV %	2.026	1.234	26	1.852	3.583	9	
Oc.S/BS %	2.767	1.124	6	2.7	1.602	4	
W. Th µm	40.143	4.18	7	35.333	9.018	3	
Os.Th µm	12	4.61	25	15	6.66	9	

* Indicates significance difference ($p \leq 0.05$) between control and irradiated group.

TABLE 5

BONE HISTOMORPHOMETRY, LUMBAR FOUR ANALYSIS, INFERIOR REGION, MEAN (X), STANDARD DEVIATION (S), AND SAMPLE NUMBER (N)

PARAMETER	IRRADIATED			CONTROL			
	X	S	N	X	S	N	
BV/TV %	25.588	4.663	28	30.475	3.9	12	*
BS/TV mm2/mm3	6.072	0.839	28	6.699	1.156	12	
Tb-Th µm	0.419	0.066	28	0.445	0.064	12	
OV/TV %	0.431	0.356	26	0.15	0.113	10	*
OS/BS %	16.158	10.24	26	4.56	2.967	10	*
OV/BV %	1.627	1.258	26	0.519	0.4199	10	*
Oc.S/BS %	3.343	2.485	7	2.033	0.723	3	
W. Th µm	44.286	11.339	7	34.333	7.371	3	
Os.Th µm	12	3.332	26	15	3.608	9	*

* Indicates significance difference ($p \leq 0.05$) between control and irradiated group.

TABLE 8

BONE HISTOMORPHOMETRY, LUMBAR FOUR ANALYSIS, ANTERIOR REGION, MEAN (X), STANDARD DEVIATION (S), AND SAMPLE NUMBER (N)

	IRRADIATED			CONTROL			
PARAMETER	X	S	N	X	S	N	
BV/TV %	24.019	10.406	28	32.244	8.975	12	*
BS/TV mm2/mm3	4.007	1.264	28	5.356	0.57	12	*
Tb-Th µm	0.574	0.093	28	0.576	0.102	12	
OV/TV %	0.238	0.206	23	0.125	0.119	10	
OS/BS %	13.965	12.862	23	3.35	3.013	10	*
OV/BV %	1.042	0.956	23	0.372	0.362	10	*
Oc.S/BS %	3.033	0.493	3	2	0.141	2	
W. Th µm	52.571	11.83	7	40	8.718	3	
Os.Th µm	12	4.569	23	21	21	10	

* Indicates significance difference ($p \leq 0.05$) between control and irradiated group.

TABLE 7

BONE HISTOMORPHOMETRY, LUMBAR FOUR ANALYSIS, POSTERIOR REGION MEAN (X), STANDARD DEVIATION (S), AND SAMPLE NUMBER (N)

PARAMETER	IRRADIATED			CONTROL			
	X	S	N	X	S	N	
BV/TV %	20.156	7.638	28	15.025	9.169	12	
BS/TV mm2/mm3	3.935	1.009	28	3.283	1.295	12	
Tb-Th µm	0.515	0.109	28	0.428	0.089	12	
OV/TV %	0.319	0.45	25	0.025	0.02	12	
OS/BS %	17.116	16.639	25	2.229	1.255	7	*
OV/BV %	1.633	1.853	25	0.1997	0.156	7	*
Oc.S/BS %	3.117	1.37	6	2.3	4.24	2	
W. Th µm	48	10.263	7	35	11.358	3	
Os.Th µm	12	3.092	26	11	1.952	7	

* Indicates significance difference ($p \leq 0.05$) between control and irradiated group.

volume (BV/TV) was significantly decreased for the irradiated group in the superior, inferior, and anterior regions. Osteoid volume (OV/BV) was significantly greater in the irradiated subjects in all regions but the superior region. However, osteoid surface (OS/BS) significantly increased in all regions in the irradiated treatment group. Osteoid volume per bone tissue (OV/TV) statistically increased for the irradiated group only in the inferior region. Bone surface (BS/TV) showed a significant decrease in the irradiated group, only in the anterior region. As far as the labeling parameters were concerned, the only observed changes were in the superior region, where the fraction of trabecular surface exhibiting double label (LAB-TS) was greater in the irradiated group (for the first set of labels), and also the bone formation rate (BFR/BS), which was calculated from the LAB-TS, was greater for the irradiated group as compared to the control. These are shown in Tables 8 through 11.

Administration of the bone labels before the irradiation dose and again prior to necropsy allows the subjects to be their own control. Therefore, a paired t-test was calculated on the adjusted appositional rate parameter (AjAR) and the only statistical significant result between the pair of labels before treatment and the pair of labels before necropsy was in the posterior region of the irradiated animals. ($p \leq 0.05$) This would also represent a significant increase in bone formation rate (BFR/BS) from the first pair of labels to the second, as bone formation rate is calculated from adjusted appositional rate. Bone formation rate (BFR/BS) has increased, in the all regions, due to the radiation treatment, but was significant in only the posterior region.

TABLE 8

BONE HISTOMORPHOMETRY, LUMBAR FOUR ANALYSIS BONE LABELING PARAMETERS, SUPERIOR REGION, MEAN (X), STANDARD DEVIATION (S), AND SAMPLE NUMBER

	IRRADIATED			CONTROL			
PARAMETER	X	S	N	X	S	N	
MD-D µm Labels 1&2	17.857	2.116	7	17.333	2.082	3	
MD-D µm Labels 2&3	27.286	8.24	7	30	12.166	3	
MD-D µm Labels 3&4	17.857	2.911	7	20.333	2.517	3	
LAB-TS Labels 1&2	0.108	0.021	7	0.067	0.004075	3	*
LAB-TS Labels 2&3	0.091	0.035	7	0.061	0.014	3	
LAB-TS Labels 3&4	0.136	0.044	7	0.082	0.016	3	
AjAR µm/day Labels 1&2	1.199	0.095	7	1.186	0.179	3	
AjAR µm/day Labels 2&3	0.359	0.11	7	0.396	0.159	3	
AjAR µm/day Labels 3&4	1.276	0.208	7	1.384	0.131	3	
BFR/BS µm3/µm2/yr Labels 1&2	47.214	8.661	7	28.961	5.799	3	*
BFR/BS µm3/µm2/yr Labels 2&3	11.758	5.102	7	8.979	4.319	3	
BFR/BS µm3/µm2/yr Labels 3&4	65.316	29.421	7	40.754	4.91	3	

* Indicates significance difference ($p \leq 0.05$) between control and irradiated group.

TABLE 9

BONE HISTOMORPHOMETRY. LUMBAR FOUR ANALYSIS BONE LABELING PARAMETERS, INFERIOR REGION, MEAN (X), STANDARD DEVIATION (S), AND SAMPLE NUMBER (N)

	IRRADIATED			CONTROL		
PARAMETER	X	S	N	X	S	N
MD-D µm Labels 1&2	17.714	3.251	7	17.333	0.577	3
MD-D µm Labels 2&3	34.571	9.71	7	19.333	11.15	3
MD-D µm Labels 3&4	17.429	1.618	7	18	1.732	3
LAB-TS Labels 1&2	0.129	0.037	7	0.083	0.019	3
LAB-TS Labels 2&3	0.114	0.04	7	0.064	0.006657	3
LAB-TS Labels 3&4	0.141	0.042	7	0.083	0.008945	3
AjAR µm/day Labels 1&2	1.188	0.18	7	1.184	0.088	3
AjAR µm/day Labels 2&3	0.455	0.127	7	0.255	0.148	3
AjAR µm/day Labels 3&4	1.245	0.116	7	1.227	0.101	3
BFR/BS µm3/µm2/yr Labels 1&2	55.482	15.865	7	35.902	8.261	3
BFR/BS µm3/µm2/yr Labels 2&3	18 968	9.19	7	6.116	3.956	3
BFR/BS µm3/µm2/yr Labels 3&4	65.408	24.292	7	37.225	3.052	3

TABLE 10

BONE HISTOMORPHOMETRY, LUMBAR FOUR ANALYSIS BONE LABELING PARAMETERS, ANTERIOR REGION, MEAN (X), STANDARD DEVIATION (S), AND SAMPLE NUMBER (N)

	IRRADIATED			CONTROL		
PARAMETER	X	S	N	X	S	N
MD-D µm Labels 1&2	17.286	1.113	7	20.333	5.859	3
MD-D µm Labels 2&3	20.167	6.401	6	17.5	3.536	2
MD-D µm Labels 3&4	17.714	2.138	7	20.333	1.155	3
LAB-TS Labels 1&2	0.107	0.035	7	0.079	0.02	3
LAB-TS Labels 2&3	0.073	0.053	6	0.086	0.035	2
LAB-TS Labels 3&4	0.107	0.036	7	0.08	0.012	3
AjAR µm/day Labels 1&2	1.166	0.096	7	1.381	0.364	3
AjAR µm/day Labels 2&3	0.264	0.082	6	0.232	0.049	2
AjAR µm/day Labels 3&4	1.265	0.153	7	1.389	0.117	3
BFR/BS µm3/µm2/yr Labels 1&2	45.527	14.855	7	39.009	9.979	3
BFR/BS µm3/µm2/yr Labels 2&3	7.837	7.859	6	6.996	1.403	2
BFR/BS µm3/µm2/yr Labels 3&4	48.832	17.126	7	40.805	8.581	3

TABLE 11

BONE HISTOMORPHOMETRY, LUMBAR FOUR ANALYSIS BONE LABELING PARAMETERS, POSTERIOR REGION, MEAN (X), STANDARD DEVIATION (S), AND SAMPLE NUMBER (N)

	IRRADIATED			CONTROL			
PARAMETER	X	S	N	X	S	N	
MD-D µm Labels 1&2	15.286	3.546	7	14.667	6.028	3	
MD-D µm Labels 2&3							
MD-D µm Labels 3&4	19.714	3.817	7	19.667	1.155	3	
LAB-TS Labels 1&2	0.092	0.031	7	0.064	0.02	3	
LAB-TS Labels 2&3	0.066	0.039	5	0.068		1	
LAB-TS Labels 3&4	0.131	0.04	7	0.163	0.107	3	
AjAR µm/day Labels 1&2	1.028	0.226	7	1.011	0.455	3	†
AjAR µm/day Labels 2&3							
AjAR µm/day Labels 3&4	1.408	0.273	7	1.345	0.135	3	†
BFR/BS µm3/µm2/yr Labels 1&2	35.14	17.143	7	23.233	9.915	3	¥
BFR/BS µm3/µm2/yr Labels 2&3							
BFR/BS µm3/µm2/yr Labels 3&4	67.669	23.008	7	83.675	63.189	3	¥

† Indicates a significant difference between the first two labels and the last two labels in the irradiated treatment group. ¥ Indicates a significant difference between the first two labels and the last two labels in the irradiated treatment group. Missing values represent no information available for that parameter.

Trabecular Pattern Measurement

Trabecular bone (cancellous bone) occupies more than 65% of the total amount of bone in the human body. The trabecular bone in the vertebra is constructed in a semi-organized structure of horizontal and vertical supporting struts called trabeculae. It is thought that there is possibly a greater loss of horizontal trabeculae when in a stressed or disease state (Vesterby et al. 1989 and Twomey et al. 1983). The possibility of preferential wasting led to the following examination as described by Twomey and associates (1983).

Three perpendicular lines are drawn on the slides that were used for the histomorphometry. One vertical and one horizontal each intersecting the midline of the vertebral body and one additional horizontal line midway between the horizontal center line and the superior bony surface as in Figure 22. The number of trabeculae intersecting each line were counted by examination through a 2X magnification microscope, and the length of each line was measured with a digital caliper. This resulted in number of trabculae per unit length. This was completed on four slides for each animal.

Results

The results were analyzed by an unpaired t-test with the standard for significance at $p \leq 0.05$. These results are tabulated in Table 12, mean (X), standard deviation (S), and sample number (N). Significance between irradiation treatment group and control group is indicated by an asterisk. The horizontal trabecular pattern measurement line (#2) that was centered in the upper quadrant was significantly decreased for the irradiated treatment group ($p=0.0085$). The one vertical trabecular pattern measurement line

TRABECULAR PATTERN MEASUREMENT

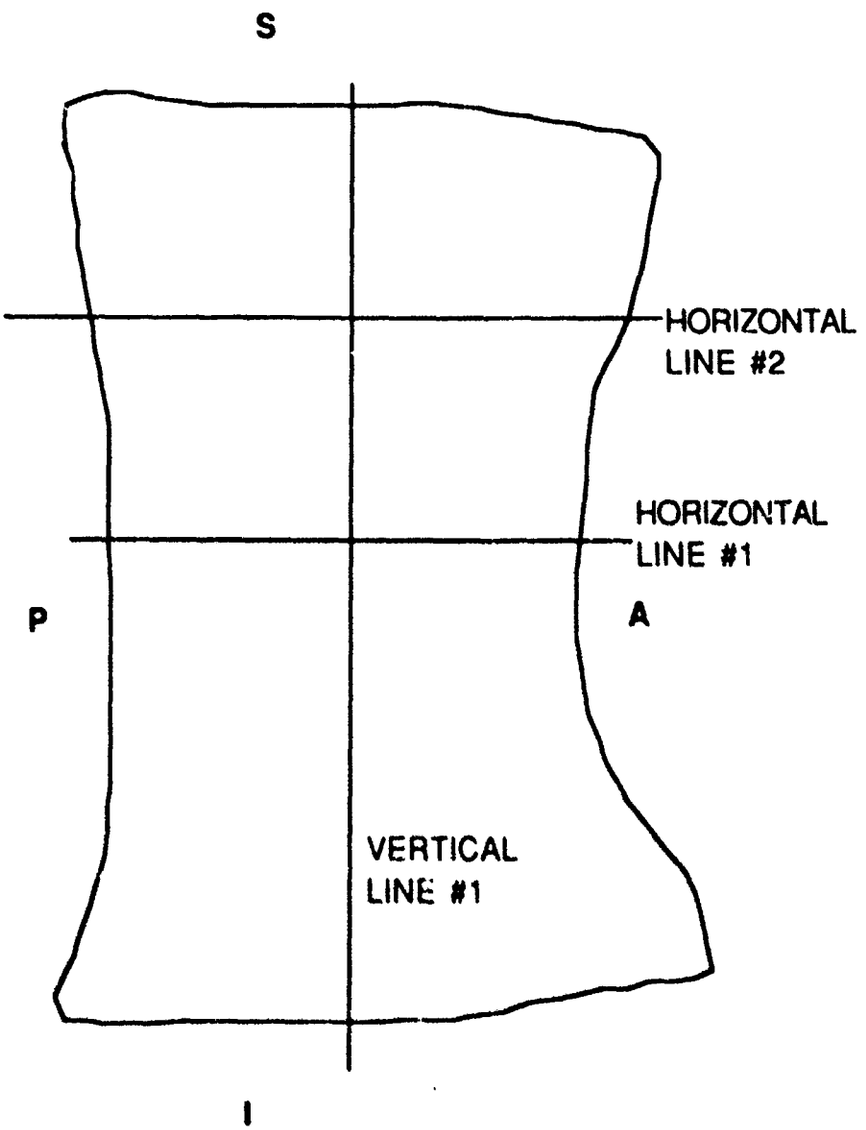

FIGURE 22. Trabecular pattern measurement analysis sites. Anatomical locations are designated anterior (A), posterior (P), superior (S), and inferior (I).

TABLE 12

TRABECULAR PATTERN RESULTS, LUMBAR FOUR, MEAN ($\bar{X}$) STANDARD DEVIATION (S), AND SAMPLE NUMBER (N)

	IRRADIATED			CONTROL			
PARAMETER	X	S	N	X	S	N	P-VALUE
Horizontal Midlin counts/mm	0.506	0.198	28	0.397	0.063	12	0.0716
Horizontal Line 2 counts/mm	1.015	0.18	28	1.198	0.213	12	0.0085
Vertical Midline	0.578	0.194	28	0.83	0.192	12	0.0005

which counts the number of horizontal trabeculae had also significantly decreased in the irradiated treatment group at a P value of 0.0005. The center horizontal trabecular pattern measurement line (#1) was not significantly different between the irradiated and control groups.

Densitometry of Radiographs

Radiographs for each of the ten animal subjects were taken before the radiation treatment and just prior to necropsy. A graded aluminum alloy wedge (0-12 mm in depth) was placed as close as possible to the lumbar level of the animal while taking the radiograph so that the image of this wedge is present on the radiograph. (See Figures 23 and 24.) With the use of this wedge image and a Scanning Densitometer (Computerized Medical Systems, St. Louis, MS-Model 8017050), densities of lumbar levels 2, 3 and 4 were to be determined. This is a procedure developed by the Clinical Radiology Testing Laboratory (Yellow Springs, OH 45387) to determine osteoporosis in patients. Wedges are sent to a radiologist along with directions for proper film exposure. The films are then sent back to the company and an assessment is made as to whether the individual has osteoporosis. In this study, the scanning densitometer scanned an area of 3 cm in width by 8 cm in length, collecting data points every 0.5 cm. An Epson computer system and a Dynascan software program was used. The scans were normalized to the wedge density reading which was the least dense, or greatest densitometry signal.

Results

Iso-density curves were plotted and analyzed by comparing percentages. The radiographs taken prior to irradiation treatment (June 1989) had percentage values ranging from 30-60% with a mode of about 50% as noted in Table 13. The radiographs that were taken on the day of necropsy (November 1989) had values around 10-20%, with the mode of 10%. There were no observed differences

Figures 23 and 24. Anterior-posterior and lateral radiographs with gradient aluminum wedge used for densitometry.

TABLE 13

DENSITY PERCENTAGE RANGES FOR RADIOGRAPHIC DENSITOMETRY MEASUREMENTS

Animal ID	Group	Pre RT %	Post RT %
JU	Irradiated	40-50%	10%
N610	Irradiated	40-50%	10-20%
N626	Irradiated	50-60%	10-20%
N630	Irradiated	40-50%	10-20%
N669	Irradiated	20-30%	10%
N680	Irradiated	40-50%	10%
N685	Irradiated	40-50%	10%
N620	Control	20-30%	10%
N626	Control	50-60%	10%
N656	Control	40%	10-20%

These percentages were normalized to the wedge.

between the irradiated group and the control group. The differences observed pre-to-post irradiation were due to the particular day (i.e. processing and radiographic technique) in which the radiographs were taken.

DISCUSSION

This study addressed several questions. First, in what way is trabecular bone responding to therapeutic dose levels of radiation? Secondly, what activity or moiety at the cellular level is affected, and is there a mechanism for repair? Thirdly, how does the resulting change at the cellular level affect the strength of the bone and ultimately the ability of the bone to overcome bone atrophy and possible fracture? The first two questions have been addressed by several authors and they all generally agree that the bone remodelling ability of the subject was compromised, however, they disagree on whether the irradiation affects the osteoblast function (formation), the osteoclast function (resorption) or both. (Cox and Moss 1989; Jacobsson et al. 1985a, 1985b, 1985c; Engstrom et al. 1987, 1983; Albrektsson 1980; Ergun and Howland 1980; Anderson et al. 1979; Rohrer et al. 1979; Friedenstein et al. 1981; and Amsell and Dell 1971, 1972) However, in all these studies, rats, mice or rabbits were used as experimental subjects. The rodent family does not undergo remodelling as the primate does. Their skeletal system is in a constant state of modeliing, as they have short lives and will continue to grow through most of it. (Hert 1972) Hopefully, this study will be able to correlate better the potential problems incurred in patients that are exposed to ionizing radiation.

The rhesus monkey (macaca mulatta) was a good experimental subject for this study. In addition to the close correlations with the human's remodelling capability, the treatment procedures for simulation and dose administration were handled very similarly as would be done for any human patient. The single dose administration was the major difference between standard human

patient treatment and the irradiation treatment of the animal subjects in this study. A fractionated dose scheme would more likely affect the bone forming cells as these are present first as osteoprogenitor cells, then osteoblasts, lining cells, and finally the more radioresistant osteocytes. An osteoblast lives approximately 54 days in contrast the osteoclast lives 2-3 days and due to this lifespan, cumulative doses to the osteoclasts would be expected to be lower than the continual dose the osteoblast could receive. (Recker 1983; and Polig and Jee 1986) However, logistical considerations did not allow for daily treatment of the animal subjects. The linear acceleration facility that was used is scheduled for patient treatment between 8 a.m. and 5 p.m. Therefore, dose administration for the subjects in this study had to take place after these hours. This study was not funded and hence, the author had to request that the veterinarian, medical physicist and radiation oncologist remain while the animals were being treated. This was an exception and would not have been practical for a six week period. Also, the radiation therapy facility is not located near the veterinary housing facility. The animals had to be anesthetized for the entire period in which they were in the hospital, and while being transported to and from the hospital. It was for these reasons that the single dose of 1300 cGy was administered instead of a fractionated regime. This was also a pilot study which was intended to set an example for further studies if necessary.

The results of the treatment planning and dosimetry reflect slightly different findings. While the treatment plan evaluates the ideal situation, the thermoluminescent dosimeter analysis reflected the possible error in system set-up. Re-creation of the irradiation treatment using a cadaver spine, water and TLDs (that cannot get wet) was not an easy task. The results illustrate these differences in the two analyses. The resultant dose from the scatter to the adjacent vertebrae is between 300 cGy (as determined from the TLDs) and 500 cGy (as determined by the treatment plan). This dose was measured with the TLDs at the center of these adjacent vertebrae and obviously the scatter would be less as the distance from the treatment field increased. The adjoining intervertebral discs, and

most likely, some of the adjacent vertebrae, (L1 and L5) were included in the direct treatment beam. This was to ensure that the treatment field did include all lumbar levels L2, L3 and L4. The dose gradient across the field from posterior to anterior was calculated to be 150 cGy in the treatment plan. The TLD analysis determined the gradient to be 550 cGy. However, the TLD measurements as stated earlier were probably flawed by misalignment and movement of the TLD chips. This could have only been verified by additional TLD measurements. The average of the anterior doses as determined by the treatment plan was 1100 cGy, therefore this will be accepted as the minimum dose given to the lumbar vertebral levels of L2, L3 and L4.

The biomechanical testing showed no statistically significant differences between the irradiated and the control group. This indicates that no significant decline in structural integrity of the vertebrae should be expected from therapeutic doses in this range at 105 days following radiation treatment. It appears that in some way the trabecular bone is still responding to the load that is applied every day to the vertebra. In the absence of physical activity, osteolysis occurs which results in bone resorption. Normally, this is minimized by the osteogenic effect of mechanical loading in accordance with Wolff's (1892) observation which states in general, "..that bone is remodelled in response to loading". The radiation effect on the trabeculae is not the same on every individual trabeculae, but there is a preferential wasting of the trabeculae that are not critical to the maintenance of the structure. Finally, the bone is responding as it would to induced loss of bone or a systemic disease state. Only one parameter showed any change. The modulus of elasticity was greater for the irradiated treatment group than for the control group ($p = 0.16$). This is not significant, but might indicate that the irradiated vertebrae have become slightly stiffer. The modulus of elasticity is a measure of the ability of a body to resist deformation.

Also supporting this biomechanical finding is the results of the analysis of the trabecular pattern measurement. Since there were volume changes in the amount of bone between the irradiated and

control groups (decrease in the irradiated group), but no change in the strength of the vertebrae in the axial direction, it was obvious that the compromise of bone loss was being made in the transverse direction. Similar results were observed in the horizontal vertebrae of elderly adult subjects (Twomey et al. 1983). Because the compression testing was completed in the axial direction, additional measurements on the vertebral slide sections were made. By a simple count of the trabeculae intersecting horizontal and vertical lines, possible conclusions could be made about the loss of bone volume and trabeculae (Twomey et al. 1983). The results of this analysis clearly indicated that there was a preferential loss of horizontal trabeculae in the irradiated vertebrae. ($p = 0.0005$) Also observed was a statistically significant difference in the upper quadrant horizontal line counts crossing the vertical trabeculae ($p = 0.0085$). Even with this great decrease in the supporting structure of the vertebral bodies, their compressive strength integrity remained intact in the axial direction.

The histomorphometric analysis gave results about what was occurring at the cellular level. The absolute amount of bone volume (BV/TV) decreased by about 4% in the superior region of lumbar four and there was a 5% decrease in the inferior analysis site ($p = 0.0188$), however, the relative changes (irradiated to control) were greater. Also, in the anterior region, the bone volume decreased by about twice as much, along with a significant decrease ($p = 0.0115$) in bone surface area (BS/TV). Since surface area was decreasing, the trabeculae were becoming thicker, but continuing to lose bone volume. Mizuno and coworkers (1976) found similar results in case analyses derived from surgical intervention. In some individuals that already were diagnosed with osteonecrosis, thicker trabeculae were found, along with an increase in the number of trabeculae. These bone volume changes also help support the conclusion that the dose to the anterior vertebra was close enough to the 1300 cGy administered dose, as predicted in the treatment plan, to cause these bone parameter changes.

Osteoid changes in response to irradiation were observed in all regions. Osteoid surface per bone surface (OS/BS) significantly

increased in all sites ($p = 0.0001$). Osteoid volume per trabecular bone volume (OV/BV) increased ($p = 0.0036$) in all but was not significant in the superior region, and osteoid volume per total bone tissue volume (OV/TV) increased significantly only in the inferior region ($p=0.0423$). These surface changes in osteoid observations can be interpreted in different ways. The fraction of the total surface occupied by a given subdivision (in this case, osteoid) is equal to the average fraction of time for which this stage of remodelling exists, providing that turnover is distributed randomly across the surface and the bone is in a steady state. Thus, between 14% and 20% of the time, osteoid is present on the surface of the bone, and bone formation is occurring 14-20% of the time in the irradiated animal subjects, increasing from the 2-7% observed in the control animal subjects. Similarly, this can be applied to the bone volume occupied by osteoid. For example, in the superior region the osteoid volume per trabecular bone volume (OV/BV) is 2%. This 2% represents the amount of time that the bone is unmineralized, and 98% of the time the bone in the superior region of lumbar 4 is mineralized. When observing the amount of osteoid present, an increase means either that activation frequency has increased or life span has increased. These are two very different conclusions drawn from one observation. The thickness of osteoid was observed in these studies. Osteoid thickness significantly decreased ($p = 0.0045$) only in the inferior region for the irradiated animal subjects, and remained unchanged in the three other regions. An increase in activation frequency or birth rate will increase the surface extent of osteoid but not the thickness, whereas an increase in life span will increase the thickness, but not the surface extent of the osteoid. In the three regions: superior, anterior and posterior there is only an increase in the surface extent of the osteoid. This would indicate that the activation frequency has increased as a result of the irradiation. The inferior region decreased in osteoid thickness, as well as increased in the surface extent of osteoid (OS/BS). This would indicate a possible change in both activation frequency and life span. Activation frequency has increased, but there is an observed decrease in life span of the osteoid. This region also showed an

increase in osteoid volume per bone volume (OV/TV), whereas the other regions did not. Perhaps in this region, activation frequency has increased as it did in the other regions, but this region is lagging behind, as indicated by the thickness of the osteoid and the increased osteoid volume per bone volume.

The information gained from bone labeling shows that there were no significant changes in fraction of double label (LAB-TS), adjusted appositional rate (AjAR) and bone formation rate (BFR/BS) between the irradiated animals and the controls. The only significant difference was in the superior region between the first two labels, which were given before any irradiation, which signifies statistical differences in the animals. There was a statistically significant difference ($p = 0.0044$) between the adjusted appositional rate (AjAR) in the posterior region between the first two labels and the second two labels (This would also include BFR/BS, as it is calculated directly from AjAR). An increase in appositional rate was observed following the radiation treatment of about 40%. The other regions also showed increases, but none statistically significant. The osteochrome is only taken up when the bone is being mineralized, and thus the increases in osteoid (unmineralized bone) may not be reflected in the bone labeling changes. However, if there were an increase in resorption prior to formation, the amount of label observed on the irradiated animals should be much less, as it should have been removed by the osteoclasts. This did not appear to be the case because there were no significant differences in the number of osteoclasts. However, the osteoclast count can be very uncertain. For one, they are very hard to identify and secondly, they have a short life in comparison to the osteoblasts. The only other way to identify resorption areas is to take measurements of the Howship's lacunae with and without osteoclasts present. This is also uncertain, as it is hard to determine if the area is truly a resorption area. Thus, authors will present this data, with its' subjectivity evident.

Conclusions in bone remodelling also rely on whether the bone is in a transient or steady state. In this case, the irradiated animals were believed to be in a transient state. As there were no changes observed in resorption, as there were in formation, it could be

concluded that resorption, which comes before formation in the A-R-F sequence, has already done its damage which resulted in an increase in activation frequency for formation as well. Whether the bone remodelling is in a steady state or not, does not matter when the object of the study is to observe differences between the treatment and control animal subjects. It is hoped that the bone remodelling would return to normal. However, once bone is lost as observed from space flight studies, there is very little chance of regaining the original bone volume or cross-sectional area (Young et al., 1986).

The radiographic density measurements demonstrated that the capabilities of radiographic determinations are limited. It was observed that there were substantial differences related to the day in which the radiographs were taken, which was presumably due to the processing and radiographic technique of the film. The company that supplies the gradient aluminum wedge sent a film chip, to ensure the proper film darkness. However, this procedure did not work in this study. Another source of error could have been due to the thickness of the vertebrae, as the standard used for the osteoporosis identification (for this company) is the index finger. However, these results were consistent with those of Rohrer and coworkers (1980) who compared radiographs, bone scans, and computed emission tomograms of rhesus monkey mandibles after 4500 cGy fractionated dose. Although histological changes were observed these clinical screening techniques found no significant changes. Therefore, other methods for density determinations would be suggested for further studies.

SUMMARY

The effects of therapeutic levels of radiation on the axial skeletal properties of the primate were examined. Ten rhesus monkeys (Macaca mulatta, 8 years old, 8.6 to 13.6 kg) were used as animal subjects. A single dose of 1300 cGy, biologically equivalent to a fractionated dose of 40 Gy was administered utilizing 6 MV photons from a linear accelerator. The specific region of lumbar levels 2, 3, and 4 were irradiated and studied. Three of the ten animals were randomly selected as control subjects. The therapeutic radiation exposure was administered to evaluate the possible clinical complications associated with atrophy of bone and subsequent osteoporosis following patient radiation treatment. In addition, these changes would be clinically relevant for the orthopaedic surgeon for procedures involving irradiated vertebrae.

Blood samples were taken to insure the general health of animals before and after treatment. A complete blood analysis was accomplished on the samples. Prior to the irradiation, radiographs were taken with an aluminum gradient wedge for densitometry measurements, and similarly just before necropsy. Bone labeling agents were administered by IV injection to both the treatment and control animal subjects for in vivo measurement of cellular changes. The bone labels (tetracycline, dicarbomethylaminomethyl fluorescein (DCAF), xylenol orange, and again tetracycline) were given before the radiation treatment and again just prior to necropsy. The treated animal subjects were sacrificed 105 days after irradiation.

Several methods for analyzing the effect of the radiation treatment were used. Firstly, compression testing was completed to determine the mechanical integrity of the bone. This perhaps is the

most important and can give more information about the possible chance of future fractures. Secondly, histomorphometric analysis was completed. With the use of bone labeling tissue-time markers, measurements of the rate of new bone formation at the bone forming surfaces was made. Thirdly, densitometric evaluation was completed on the radiographs. Finally, a trabecular bone pattern measurement was taken on the individual slides used for the histomophometry. This was used to help substantiate the hypothesis that preferential wasting of the horizontal trabeculae was occurring, and is a mechanism for the bone to maintain its compressive strength, while continuing to lose bone volume. In addition to the analyses to determine the changes in the structural and cellular integrity of the bone, radiation dosimetry was used to assess the dose administered to the selected lumbar levels. Both computer assisted treatment planning and thermoluminescent dosimetry (TLD) were used to evaluate the actual doses administered.

The TLD analysis was completed with five strips of five pairs of TLDs. Each strip was placed on the vertebra in these locations: anterior aspect of the spine, left and right lateral aspect of the spine, and left and right posterior aspect of the spine. Each pair of TLDs were located on a given vertebrae: L1, L2, L3, L4, and L5. Lumbar levels 2, 3, and 4 were irradiated with 1300 cGy based on the computerized treatment plan. Thermoluminescent dosimetry evaluation suggested that the dose to the vertebra (L2, L3, and L4) to range between 738 cGy and 1300 cGy, at the anterior of the vertebra. However, this range was affected by errors in TLD placement and phantom positioning. Scatter to the adjacent vertebrae (L1 and L5) was approximately 300 cGy.

Compression testing was completed on lumbar levels two and three at a rate of 210 in/min to a 50% reduction in height of the vertebrae. All processes were removed, along with soft tissue so that only the centrum remained. All centra were tested axially. There were no significant differences between the irradiated and the control animal subjects in any of the strength parameters.

Histomorphometric analysis was completed on lumbar level four. Four slides were prepared for each animal and four analysis

sites were examined on each slide: superior, inferior, anterior and posterior. The following parameters were chosen to represent the overall remodelling changes in the bone: bone volume per tissue volume, bone surface per tissue volume, trabecular thickness, wall thickness of trabeculae, osteoid thickness, osteoid volume per tissue volume, osteoid volume per trabecular bone volume, osteoid surface per bone surface, number of osteoclasts per bone surface, mean distance between double label, fraction of surface containing double label, adjusted appositional rate and bone formation rate. The latter four were determined from the bone labeling agents administered. A significant decrease in bone volume was observed in the anterior, inferior, and superior analytical sites. Bone surface per tissue volume also significantly decreased in the anterior region. Osteoid surface per bone surface significantly increased in the irradiated animal subjects for all four analytical regions. Osteoid volume per trabecular bone volume increased in all but the superior region, and osteoid volume per bone tissue volume increased only in the inferior region. Adjusted appositional rate (as well as bone formation rate which is directly calculated from adjusted appositional rate) significantly increased by 40% in the posterior region in the irradiated subjects. This was measured by determining the differences between the first two labels and the last two labels. There was also a significant difference in the fraction of double label per bone surface between the treatment and control in the superior analysis site, as observed with the first two labels. This difference can only be due to the lack of similarity in animals, as no radiation dose was given at this time.

The radiographic density analysis was not useful in determination of bone density loss. This was either due to a limited ability of this type of analysis to resolve modest density changes, or the thickness of the vertebrae and the surrounding soft tissue reduced the sensitivity of this type of analysis.

The trabecular pattern measurement showed a decrease in the number of horizontal supporting trabeculae, as well as a decrease in the vertical trabeculae in the upper quadrant. This final analysis helped substantiate the hypothesis that the vertebrae ca maintain

it's axial strength by continuing to maintain the individual vertical trabeculae, but decreasing the number of horizontal trabeculae while a loss in bone volume is taking place. The conclusion that there is preferential wasting is evident. This is very important in the clinical situation, as it indicates that even though bone is being lost, strength is not compromised. Consequently, the chance of fracture is lessened in the trabecular bone that has been irradiated. This study only measured changes in vertebra, and specifically the lumbar vertebra of levels 2, 3, and 4 at 105 days post RT. The same conclusion could not necessarily be drawn for cortical bone, and possibly not for the rest of the vertebra either. The entire vertebral column is not straight, and therefore not in absolute axial compression. This must be taken into account when making similar conclusions concerning other vertebrae. However, it is likely the same preferential wasting would occur in other vertebrae, following irradiation treatment. In addition, when examining late effects of radiation one actually studies the daughter cells that are several generations removed from the irradiated precursor cells. The irradiation may impair the normal cellular activity for several generations. Additional changes in bone remodelling could take place following this 105 day observation period or normal bone turnover could follow, as observed by Deffebach and Phillips (1968) at 5+ years post RT on the eleventh thoracic vertebra.

In conclusion, local irradiation of the lumbar levels of 2, 3, and 4 to a therapeutic dose level brings upon changes in the bone remodelling, specifically observed as activation frequency and formation, and that these changes occur preferentially in the horizontal trabeculae while maintaining the strength of the vertebral centrum.

REFERENCES

Aitasalo, K and M Neva. Morphometry of orthopantomographic mandibular bone changes during radiation therapy. Acta Radiologica Diag 26:551-556, 1985.

Albrektsson, T. Repair of bone grafts. A vital microscopic and histologic investigation in the rabbit. Scan J Plast Reconstr Surg 14:1, 1980a.

Albrektsson, T, M Jacobsson, and I Turesson. Irradiation injury of bone tissue. Acta Radiol Oncol 19:235-239,1980b.

Albrektsson, T, M Jacobsson and I Turesson. Bone remodelling at implant sites after irradiation injury. Swedish Dent J, Supp. 28: 193-203, 1985.

Albright, JA and RA Brand. The Cell- The Scientific Basis of Orthopaedics. Appleton-Century-Crofts, New York, pp. 1-21, 1979.

Amsell, S and ES Dell. Response of the preosteoblast and stem cell of rat bone marrow to a lethal dose of x-radiation or cyclophosphamide. Cell Tiss Kinet. 4:255-261, 1971.

Amsell, S and ES Dell. Bone formation by hemopoietic tissue: Separation of preosteoblast from hemopoietic stem cell function in the rat. Blood 39(2):267-273, 1972.

Anderson, MD, RA Colyer and LH Riley. Skeletal changes during prolonged external irradiation: Alternations in marrow, growth plate and osteoclast population. The Johns Hopkins Medical Journal 145:73-83, 1979.

Aronson, AS, M Gustafson and G Selvik. Bone growth in the rabbit after radiation. Acta Radiologica Diag. 17:838-844, 1976.

Babicky, A and J Kolar. Generalized skeletal response to local radiation injury. Rad Res. 27:108-118, 1966.

Barnhard, HJ and RW Geyer. Effects of X-radiation on growing bone. Radiology 78:207-214, 1962.

Beddoe, AH. A quantitative study of the structure of trabecular bone in man, rhesus monkey, beagle and miniature pig. Calcif Tiss Res 25:273-281, 1978.

Bures, MF and AH Wuehrman. Bone-remodeling dynamics following local X irradiation: I. J Dental Res. 48:376-384, 1969.

Cox, JD, RW Byhardt, JF Wilson, JS Haas, R Komaki and LE Olson. Complications of radiation therapy and factors in their prevention. World J Surg 10:171-188, 1986.

Cox, JD and WT Moss, ed. The Bone. In: Radiation Oncology: Rationale, Technique, Results. CV Mosby Company, St Louis, pp. 683-701, 1989.

Crone-Munzebrock, W and RP Spielman. Quantification of recalcification of irradiated vertebral body osteolyses by dual-energy computed tomography. Europ J Radial. 7:1-5, 1987.

Dalinka, MK, J Edeiken and JB Fenkelstein. Complications of radiation therapy: Adult bone. Semin Roentgenol 9:29-40, 1974.

Dambrain, R, A Dhem, J Gueulette, and A Wambersie. Bone vitality in the cat's irradiated jaw: Histological study. Strahlentherapie Und Onkologie 164(6):351-356, 1988.

Deffebach, RR and TL Phillips. Benign osteoblastoma of the vertebra. Radiol Clin Biol 37:45-52, 1968.

Engstrom, H. Effects of irradiation on growing bones. Swedish Dental J. 45(1):1-47, 1987.

Engstrom, H, JO Jansson and C Engstrom. Effects of local irradiation on longitudinal bone growth in the rat. Acta Radiol Oncol 22:129-133, 1983.

Ergun, H and WJ Howland. Postradiation atrophy of mature bone. In: CRC Crit Rev Diagn Imaging CRC Press, Inc., Boca Raton, pp. 225-243, 1980.

Ewing, J. Radiation osteitis. Acta Radiol 6:399-412, 1926.

France, EP. Effects of acute hypogravic exposure and recovery on the vertebral column of juvenile primates (Macaca mulatta). Doctoral Thesis, Wright State University, Dayton, Ohio, 1984.

Friedenstein, AJ, NV Latzinik, UF Gorskaya, and SY Sidorovich. Radiosensitivity and postirradiation changes of bone marrow clonogenic stromal mechanocytes. Int J Radiat Biol 39:537, 1981.

Frost, HM. Bone Remodelling Dynamics. Charles C. Thomas, Springfield, IL, 1963.

Frost, HM. Tetracycline-based histological analysis of bone remodelling. Calcif Tiss Res. 3:211-237, 1969.

Frost, HM Bone Modelling and Skeletal Modelling Errors. CC Thomas, Springfield, IL, 1973.

Frost, HM. A determinant of bone architecture. Clin Orthop. 175:286-292, 1981.

Frost, HM. Bone Histomorphometry: Choice of marking agent and labeling schedule. In: Bone Histomorphometry: Techniques and Interpretation. Recker, RR., ed., CRC Press, Inc., Boca Raton, pp. 37-53, 1983.

Hardt, AB. Modification of the tape-transfer technique: Reduced shattering and distortion of hard tissue sections. J Histotechnology 9(4): 253, 1986.

Hert, J, E Pribylova and M Liskova. Reaction of bone to mechanical stimuli. Part 3: Microstructure of compact bone of rabbit tibia after intermittent loading. Acta Anat 82:218-230, 1972.

Horowitz, YS. , ed. Thermoluminescence and Thermoluminescent Dosimetry, Volume II. CRC Press, Inc., Boca Raton, pp. 2-3, 1984.

Howland, WJ, RK Loeffler, DE Starchman and RG Johnson. Postirradiation atrophic changes of bone and related complications. Radiology 117:677-685, 1975.

ICRU Report 24. Determination of absorbed dose in a patient irradiated with beams of x and gamma rays in radiotherapy procedures. International Commission on Radiation Units and Measurements. Washington D.C., 1976.

Jacobsson, MG, AK Jonsson, TO Albrektsson, and IE Turesson. Alterations in bone regenerative capacity after low level gamma irradiation. Scand J Plast Reconstruc Surg 19:231-236, 1985a.

Jacobsson, MG, AK Jonsson, TO Albrektsson and IE Turesson. Dose-response for bone regeneration after single doses of ^{60}Co Irradiation. Int J Rad Oncol 11:1963-1969, 1985b.

Jacobsson, MG, TO Albrektsson, and IE Turesson. Dynamics of irradiation injury to bone tissue. A vital microscopic investigation. Acta Radiol Oncol 24:343-350, 1985c.

Jacobsson, MG, AK Jonsson, TO Albrektsson and IE Turesson. Short and long-term effects of irradiation on bone regeneration. Plast Reconstr Surg 76:841-848, 1985d.

Jacobsson, MG, P Kalebo, A Tjillstrom and IE Turesson. Bone cell viability after irradiation. Acta Oncol (Sweden) 26(6):463-465, 1987.

Jee, WSS. The influence of reduced local vascularization on the rate of internal reconstuction in adult long bone cortex. In: Bone Biodynamics, HR Frost, ed., Boston, p. 259, 1984.

Kazarian, LE and HE von Gierke. Bone loss as a result of immobilization and chelation. Clin Orthop 65: 67-75,1969.

Kazarian, LE and I Kaleps. Mechanical and physical properties of the human intervertebral joint. AMRL-TR-79-3, 1979.

Kazarian,LE and HE von Gierke. The effects of hypokinesia in primates on bone strength. Acta Astronaut 8:1075-1082, 1981.

Leichter, I, A Bivas, A Giveon, JV Margulies and A Weinreb. The relative significance of trabecular and cortical bone density as a

diagnostic index for osteoporosis. Phys Med Biol 32(9):1167-1174, 1987.

Mack, P, P LaChance, G Vose and F Vogt. Bone demineralization of foot and hand of Gemini-Titan IV, V and VII astronauts during orbital flight. Am J Roentgenol 100:503-511, 1967.

Malluche, HH, D Sherman, M Wolfgang and SG Massry. A new semiautomatic method for quantitative static and dynamic bone histology. Calcif Tissue Int 34:439-448, 1982.

Maeda, M, MH Bryant, M Yamagata, G Li, JD Earle, EYS Chao. Effects of irradiation on cortical bone and their time-related changes. J Bone Joint Surg 70-A(3):392-399, 1988.

Mizuno, A, M Shimizu, and T Ueno. Histopathologic and roentgenographic studies on the effects of irradiation on the human mandibles. Bull Tokoyo Dent Univ 23:179-201, 1976.

Parfitt, AM. The physiologic and clinical significance of bone histomorphometric data. In: Bone Histomorphometry: Techniques and Interpretation. Recker, RR., ed., CRC Press, Inc., Boca Raton, pp. 143-217, 1983a.

Parfitt, AM. Stereologic basis of bone histomorphometry: Theory of quantitative microscopy and reconstruction of the third dimension. In: Bone Histomorphometry: Techniques and Interpretation. Recker, RR. ed., CRC Press, Inc., Boca Raton, pp. 53-88, 1983b.

Parfitt, AM. Bone histomorphometry: Standardization of nomenclature, symbols and units. Summary of proposed system. Bone Miner 4(1): 1-5, 1988.

Parker, RG and HC Berry. Late effects of therapeutic irradiation on the skeleton and bone marrow. Cancer 37: 1162-1171, 1976.

Podenphant, J and U Engel. Regional variations in histomorphometric bone dynamics from the skeleton of an osteoporotic women. Calcif Tissue Int 40:184-188, 1987.

Pope, NS, KG Gould, DC Anderson and DR Mann. Effects of age and sex on bone density in the rhesus monkey. Bone 10:109-112, 1989.

Powers, BE, EL Gillette and SL McChesney. Response of canine lumbar vertebrae to intraoperative irradiation. Abstracts, 36th Annual meeting of the Radiation Research Society, Philadelphia, PA, April 16-21, 1988., pg 131.

Rafii, M, H Firooznia, C Golimbu and N Horner. Radiation induced fractures of sacrum: CT diagnosis. J Comp Assist Tomo 12:231-235, 1988.

Recker, RR. Bone Histomorphometry: Techniques and Interpretation. CRC Press, Inc., Boca Raton, 1983.

Rohrer, MD, Y Kim, and JV Fayos. The effect of cobalt-60 irradiation on monkey mandibles. Oral Surg 48(5):424-440, 1979.

Rohrer, MD, LT Kircos, JH Thrall, Y Kim, and JV Fayos. Evaluation of irradiated mandibles using emission tomography, bone scans, and radiography. J Dent Res 59(12):2032-2037, 1980.

Rubin, P, R Andrews, R Swarm and H Gump. Radiation induced dysplasia of bone. 82:206-216, 1959.

Saha, S. Short-term and long-term effects of irradiation on bone regeneration-A discussion. Plast Reconstr Surg 76:849-850, 1985.

Sams, A. The effect of 2000 r of x-rays on the acid and alkaline phosphatase of mouse tibiae. Int J Rad Biol 10(2):123-140, 1965.

Schantz, A, AL Schiller and SP Kadish. Localized aplasia in irradiated vertebral bone marrow: A frequently overlooked gross observation. Arch Path 92:187-190, 1971.

Sengupta, S, and K Prathap. Radiation necrosis of the humerus, a report of three cases. Acta Radiologica (Ther) 12:313-319, 1973.

Sontag, MR and JR Cunningham. Corrections to absorbed dose calculations for tissue inhomogeneities. Med Phys 4:431, 1977.

Spencer, RP, JR Arnow, N Kayani and H Kassamali. Vertebral "void" on radiogallium imaging after radiation therapy. Clin Nuc Med 13:303-304, 1988.

Swenson, KN. A study of the histomorphometry of the talus following low frequency vibration. Masters Thesis, Wright State University, Dayton, Ohio, 1987.

Twomey, L, J Taylor and B Furniss. Age changes in the bone density and structure of the lumbar vertebral column. J Anat 136:15-25, 1983.

Van Audekercke, R and M Martens. Mechanical properties of cancellous bone. In: CRC Natural and Living Biomaterials. CRC Press, Boca Raton,pp. 89-98, 1984.

Vaughan, J. The effects of skeletal irradiation. Clin Orthop 56: 283-303, 1968.

Vesterby, A, HJG Gundersen, and F Melson. Star volume of marrow space and trabeculae of the first lumbar vertebrae: Sampling efficiency and biological variation. Bone 10:7-13, 1989.

Villaneueva, AR and KD Lundin. A versatile new mineralized bone stain for simultaneous assessment of tetracycline and osteoid seams. Stain Technology 64(3): 129-138, 1989.

Werts, ED, MJ Johnson, and RL DeGowin. Postirradiation hemopoietic repopulation and stromal cell viability. Radiat Res 71: 214-224, 1977.

White, DR, HQ Woodard, and SM Hammond. Average soft-tissue and bone models for use in radiation dosimetry. Br J of Radiol 60: 907-913, 1987.

Withers, HR. Some changes in concepts of dose fractionation over 20 years. Front Radiat Ther Onc 22:1-3, 1988.

Wolff, JD. Das Gesetz der Transformation der Knochen. Berlin, 4. Hirschwald, pp. 1-152, 1892.

Young, DR, WJ Niklowitz, RJ Brown, and WSS Jee. Immobilization-associated osteoporosis in primates. Bone 7:109-117, 1986.

APPENDIX 1

Rhesus Monkey Reference Values

HEMOGRAM		
Red Blood Cell (RBC)	4.33-6.75	/pL
Hematocrit (HCT)	31.9-49.0	%
Hemoglobin (HGB)	10.4-15.8	g/daL
Mean Corpuscular Volume (MCV)	67.3-78.8	fL
Mean Corpuscular Hemoglobin (MCH)	21.3-26.3	pg
Mean Corpuscular Hemoglobin Concentration (MCHC)	30.6-34.4	g/daL
White Blood Count (WBC)*	2.66-14.3	/nL
Neutrophils	25-95	%
Lymphocytes	0-70	%
Monocytes*	0-7	%
Eosinophils*	0-4	%
Basophils*	0-0	%
Platelets	152-558	/nL

*Not normally distributed

APPENDIX 2

Glossary of Terms*

a/ß ratio-is equal to the dose D when cell killing in linear and quadratic terms are equal on a cell survival curve

acid phosphatase-a chemical found in bone and blood chemistries generally associated with bone resorption

activation-stimulation of cell division and bone remodelling to take place by an unknown agent or stimulus

alkaline phostphatase-a chemical found in bone and blood chemistries generally associated with bone formation

atrophy-a wasting of tissues, diminished cell proliferation

BMUs-(Basic Multicellular Units) individual remodelling packets that undergo the bone remodelling sequence together

bone marrow-the soft, fatty substance filling the medullary cavaties and spongy extremities of the long bones

calcification front-the interface between the mineralized and unmineralized bone

cancellous bone-denoting bone that has a lattice-like or spongy structure

cement line-the interface where the bone resorption perimeter has stopped and formation has begun to fill in bone

compact bone-also known as cortical bone, generally found in the appendages and surrounding all other bone

formation-following resorption, it is the final stage in the A-R-F sequence of bone remodelling, where new bone is laid down in the area where resorption had taken place

hematopoeitic-(hemopoietic) pertaining to or related to the formation of blood cells

Howship's lacunae-a cavity where bone resorption has taken place and the bone has been removed, denoted by a scalloped border

in situ-in position

in vivo-in the living body, referring to a process or reaction therein

in vitro-in an artificial environment (i.e. test tube or culture media)

labeling-the use of an identifiable substance which deposits in bone tissue, and thus the amount of bone deposition can be measured

lamellar bone-bone that has been deposited following resorption, and is arranged in thin plates or scales

lining cells-previously called resting osteoblasts, lining cells are osteoblasts that have completed forming bone in a particular area and have now taken a flat oblong shape (end stage cells)

lytic-the destruction of red blood cells, bacteria or other antigens by a specific lysin

mineralization-the process where unmineralized bone is calcified, approximately 10-20 days following bone matrix deposition

modelling-bone growth occurring on the periosteal surface, primarily growth

necrosis-irreversible death of a tissue

osteitis-inflammation of bone

osteoblast-columnar or cuboidal cells with basophilic cytoplasm arranged in a continual one cell thick sheet that lays down the matix of unmineralized bone

osteochrome- a bone labeling agent when in high blood level concentrations becomes accessible to all free bone srufaces and becomes encorporated into the mineralization front and remains in the bone until resorption removes it- an osteochrome will fluoresce when under ultraviolet light

osteoclast-a large, multinucleated cell with ruffled borders and abundant acidophilic cytoplasm that solubize mineralized bone and remove it

osteocytes-osteoblasts that were recently entombed in the mineralized bone, and can continue to form new bone around them for a period of time until the endosteal resorbing surface comes closer and death occurs shortly before being resorbed

osteoid-bone matirx that has been formed, but is not yet mineralized

osteopenia-decreased calcification of density of bone

osteopetrosis-charaterized by absence of osteoclasts resulting in thickened and dense trabecular bone and calcified cartilage leading to decreased marrow space and anemia

osteoporosis-reduction in the quantitiy of bone or atrophy of skeletal tissue, resulting in trabeculae that are scanty and thin

osteoprogenitor cell-more differentiated from a stromal cell and possibly present during the quiescent or remodelling stage, this cell will become an osteoblast

osteosclerosis-abnormal hardening of bone

preosteoblast-a precursor cell or line of cells residing in hemopoeitic tissue that has the potential to differentiate into an osteoblast and form bone

remodelling-growth and resorption occurring on the endosteal surface, where bone touches marrow

resorption-the second in the A-R-F bone remodelling sequence where bone is removed

sigma-the time duration for the sequence of remodelling events to take place

trabeculae-a small piece of the spongy substance of bone usually interconnected with other similar pieces; the supporting structures of bone forming a lattice

trabecular bone-bone that contains trabeculae, located in the vertebrae, pelvis and the head of the femur

*Some of these definitions were taken from Stedman's Medical Dictionary, 24th Ed., Williams and Wilkins, Baltimore, MD, 1982.